

5.3.4 Central Span Length of the Main Bridge

The required central span length of the main bridge can be determined by the required horizontal navigational clearance and the magnitude of structure required from assessing the conditions that the bridge structures (abutments and piers) are stable and safe from hydrodynamic issues such as riverbed change and local scouring around the foundations. The required central span length is governed by hydrodynamic issues rather than the horizontal navigational clearance (300 m), and the requirements from the hydrodynamic and economic viewpoints are discussed as below.

- The right riverbank 7 km upstream of the route faces the river stream and erosion has occurred at a rate of 3 m/year from 1972 to 1993 (according to the satellite image analysis).
- The left riverbank 4.5 km upstream of the route faces the river stream and erosion has also occurred.
- Immediately upstream of the route, the riverbed has deepened. This riverbed deepening may be related to the planform (riverbank) changes at the upstream river sections previously described.
- At the river section (1 km downstream from the existing ferry and 1.9km upstream from the bridge crossing), the left side (outside of the river flow) riverbed has increased in depth up to 28 m from 1961 to 1997.
- At the river section where the route crosses, the riverbed has become deeper year by year. This was recognized from the changes in the maximum river water depths of 13 m, 17 m, and 19 m in the years 1963, 1991, and 1997/1998, respectively.
- At the river section of the route, an increase of velocity (1.21 m/sec June 1998) was observed from the left riverside to the middle of the river, the peaking of velocity was at approximate 350 m from the left riverbank. This velocity peak location (observed in June 1999) may considerably affect the hydrodynamic issues around the pier foundation if the pier is near this point.

Consequently, to avoid the hydrodynamic issues around the pier foundation and to maintain more safety of bank clearance to the maneuvering lane for large size vessels, the central span length of the main bridge should be 550 m from the left riverbank where one main tower foundation will be constructed, compared with 500m in the Feasibility Study.

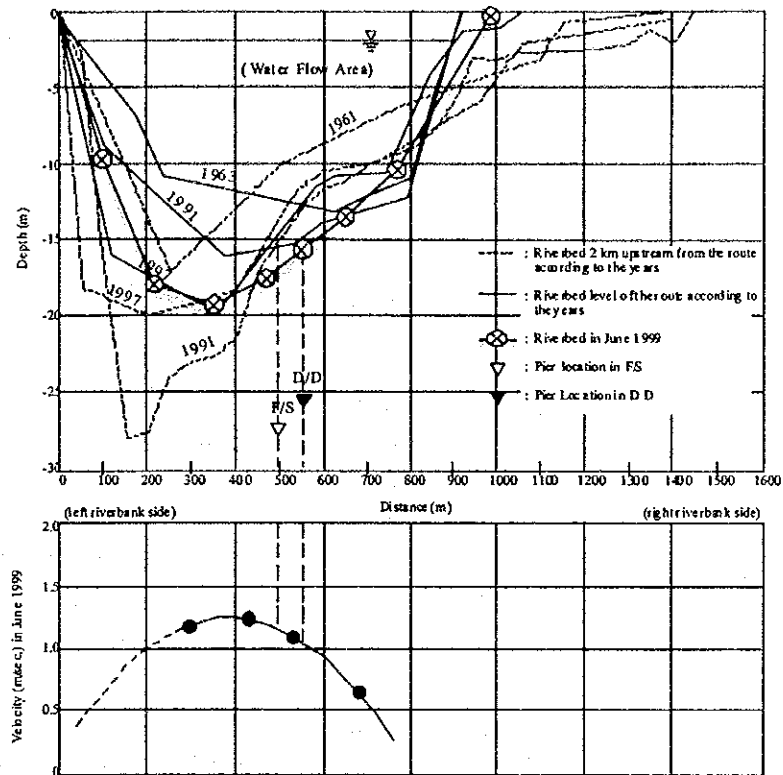


Figure 5.13 Riverbed Change and Flow Velocity

5.3.5 Location of Tower on the Left Riverbank for the Main Bridge

The location and the foundation depth of the tower on the left riverbank were decided from the following reasons: to maintain the maneuvering safety for large size vessels by locating the tower pier on the land, which is also able to economize construction costs compared with constructing the tower pier in the river, to support the foundation stability in case of the riverbank erosion by extreme floods in the futures, and to avoid hydrodynamic problems such as local scouring it may occur around the pier foundations in case that the pier was constructed in the deep stream of the Hau River.

5.3.6 Type and Structural Layout of the Main Bridge

(1) Type of the Main Bridge

The required central span length is not less than 550m, which is estimated based the horizontal navigational clearance, hydrodynamic issues and riverbed change. The possible bridge types corresponding to the applicable span length are as follows:

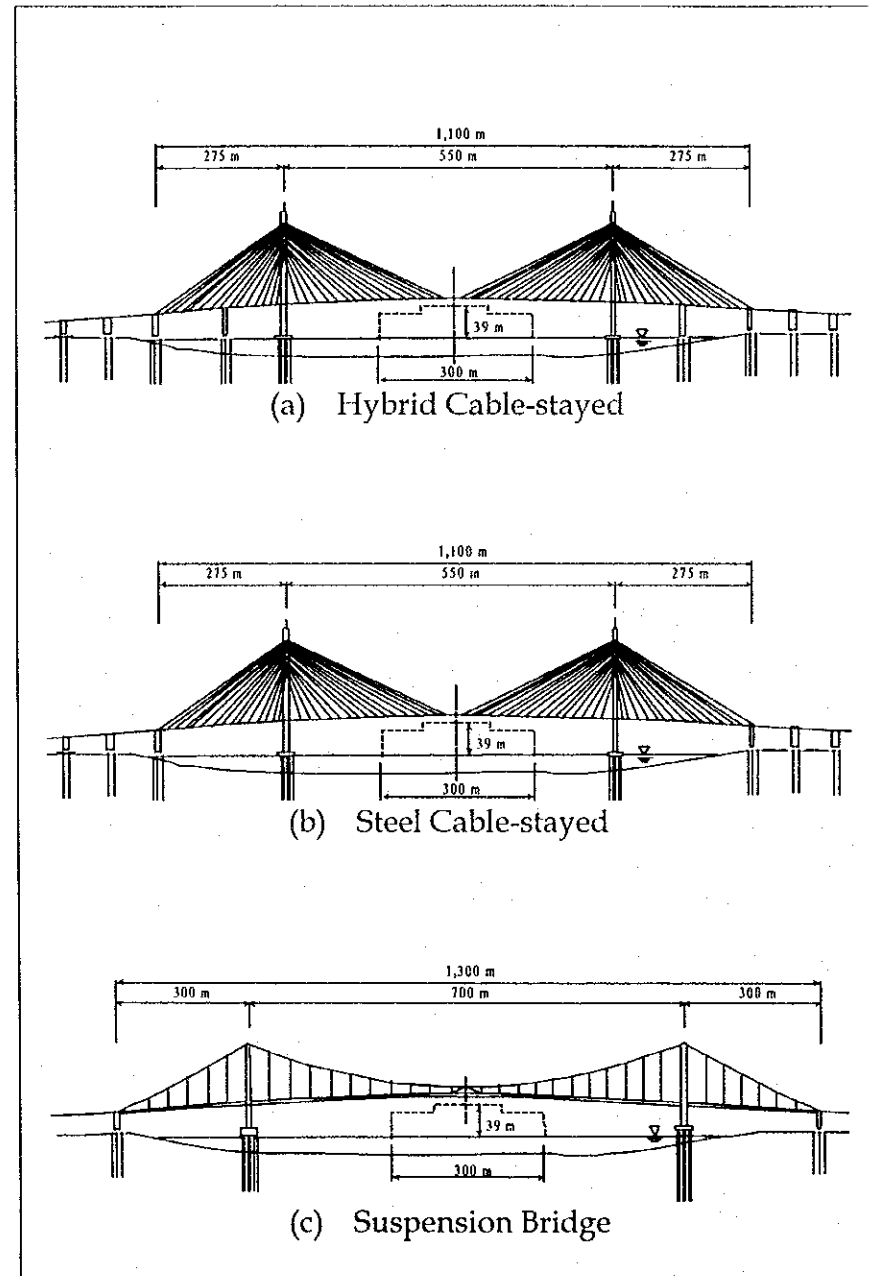
Table 5.4 Bridge Type of the Main Bridge

Bridge Type	Applicable Span Length (m)
a) Hybrid Cable-Stayed	350 ~ 800
b) Steel Cable-Stayed	> 550
c) Steel Suspension Bridge	> 650

A Hybrid Cable-stayed bridge for the main span is recommended for the following reasons:

- The Hybrid (steel and concrete) bridge types can maximize using construction materials locally procured, which can economize the bridge construction cost compared with an all steel bridge type.
- The longer span of the Hybrid Cable-stayed bridge type can minimize the number of piers where the foundations have to penetrate into the bearing stratum approx. 100 meters deep.
- The Hybrid Cable-stayed bridge type is applicable to longer spans, that means it is able to minimize hydrological and hydraulic problems such as river bank erosion, local scouring erosion of piers. It provides the required horizontal navigational clearance, and can minimize the girder depth for the higher vertical navigational clearance (39.0m)
- The cable-stayed bridge with a partial concrete structure (hybrid system) can be advantageous in the case of aerodynamic stability compared with all steel structure.
- The towers and cables provide symbolic and landmark views, and are aesthetically pleasing.

Table 5.5 Comparative Bridge Types for the Main Bridge



Description	(a) Hybrid (PC) Cable-Stayed Bridge	(b) Steel Cable-Stayed Bridge	(c) Suspension Bridge
Economy	- Cost is higher than PC cable-stayed. - Provides a longer span than PC cable-stayed bridge because of lightweight of construction of the steel girder in the central span.	- Girder is steel structure and applicable to longer span. - Cost is higher than PC hybrid cable-stayed type.	- The most expensive bridge type - This type is used only the case that it is necessary to cross the full width of the river.
Structural Features	- Flexible structural system and ductile system. - Dead weight of central girder is light and steel structure, and side spans are prestressed concrete to be heavy weight of counter span.	- Flexible structural system leads difficulty to induce transferred stress and adjust stay cable. - Light dead weight of girder can be applied to long center span.	- Anchorage will be huge structure due to soft subsoil and deep bearing strata. This is a major disadvantage of suspension bridge.
Construction	- Erection is done by free cantilever method. - Girder elements are prefabricated as precast segments and assembled by the erection nose. Transportation of segments is done by pontoon. Approach viaducts are erected from one-way with gantry crane and launching girder.	- Erection is done by free cantilever method. - Girders can be prefabricated. - Adjusting stress of cable stays is more difficult during cantilever construction due to no fixed point.	- Main piers are located in the land area, this means easier construction can be expected.
Maintenance	- Girders made from prestressed concrete are maintenance free, however center span is necessary to be maintained for preventing from corrosion.	- For maintenance and to prevent corrosion of girder and stay cable, it is necessary to repaint steel girders.	- Cable and hanger should be maintained and steel girder will be also repainted periodically.
Aesthetic Aspect	- This type of bridge is both symbolic and landmark.	- This type of bridge is both symbolic and a landmark.	- This type bridge is both symbolic and be landmark.

PC: Prestressed Concrete
 Hybrid: The bridge deck is a combination of steel and concrete structures i.e. steel structure for middle part of central span and concrete structure for the remained parts of central span and side span

Rating Marks
 ⊙ Excellent
 ○ Good
 Δ Fair
 × Bad

Evaluation by Marks

Description	(a)	(b)	(c)
Economy	○	Δ	×
Structural Features	⊙	Δ	○
Construction	○	Δ	Δ
Maintenance	Δ	×	×
Aesthetic Aspect	○	○	⊙
Result	⊙	○	○

(2) Optimum Steel Girder Length in the Central Span

To optimize the steel girder length in the central span of the main bridge, the following items were compared:

- Maximum and minimum bending moment
- Forces active at the junction of steel and concrete girders
- Deflection magnitude of the mid-span from live loads
- Reaction forces at the tower foundations
- Number of supplement any piers for the side spans
- Construction cost ratio

Consequently, the case with the 210m steel girder length is recommended for the following reasons.

- Structural output such as bending moment, deflection, etc., are minimal compared to other cases.
- Construction cost is comparatively cheap.
- Even though two piers are required for the side spans, providing these piers improves the total stability of the structure.

(3) Shape of Girder Section

There are three possible shapes of the girder section for the main bridge: a) Edge Girder Type, b) Triangle Edge Girder with Stiffner, and c) Trapezoidal Box Type.

a) Edge Girder Type:

Torsional rigidity of the main girder is smaller. Since the hanging point of cable is at the gravity center, the girder itself is stable. Due to smaller rigidity, deflection of girder by live load is greater.

b) Separated Trapezoidal Box:

The section area of the girder and geometrical moment of inertia is smaller, which can make the bending moment of the girder smaller. The deflection of this girder type is greater than that of trapezoidal box type, by up to a factor of 2 times.

c) Trapezoidal Box Type:

Since the girder section is of the closed type, the torsional rigidity and geometrical moment of inertia are greater and more stable type for aerodynamic behavior. It has advantages of precast segmental construction and the hybrid system girder.

Trapezoidal Box Type is recommended from the technical and economical viewpoints of aerodynamic stability, segmental construction, and hybrid system of girder.

Table 5.6 Shape of Girder Section

	Section of Girder	Structural Feature	Remarks
<p>Alternative-3 Edge Girder Type</p>		<p>Floor beam is necessary in short interval, and manufacture of a segment is complicated. Unstable at joint structure between concrete and steel structures. Balance for wind is a subject. Unit Weight of PC-Girder $W = 58.7$ tf/m</p>	
<p>Alternative-2 Separated Trapezoidal Box Girder with Stiffner</p>		<p>Floor beam is necessary in short interval, and manufacture of a segment is completed. Hardness joint is difficult. For a section of trapezoid, balance for wind is inferior. Unit Weight of PC-Girder $W = 43.1$ tf/m</p>	
<p>Alternative-1 Trapezoidal Box Shape</p>		<p>Manufacture of segment is easy. Good balance for wind. Joint structure is easy. Flexural rigidity and torsional rigidity are hard. Unit Weight of PC-Girder $W = 44.9$ tf/m</p>	<p>recommended</p>

(4) Shape of Tower

The shape of tower for the cable-stayed bridge can be divided into two shapes, H-shape and A-shape.

From the reasons of the structural stability, A-shaped tower is superior for longer span bridge because the inclined cables can resist torsional behavior of the bridge deck. The degree of deformation for each shape is schematically shown as below. The A-shape tower is recommended as the tower shape of the main bridge.

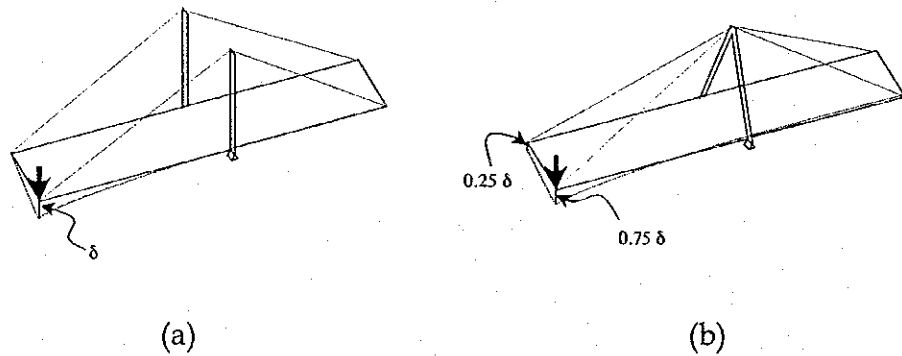


Figure 5.14 Shape of Tower

As shown in Figure 5.15, typical (a) and modified A type towers (b) and (c), typical A shape is the smallest deformation and bending moment at the bottom due to lateral loads like wind or earthquake forces. Furthermore, influence to the foundation is the least in the case of typical A type (a).

The configurations of the typical A types are shown as below. Among them, the same type as the Feasibility Study is recommended.

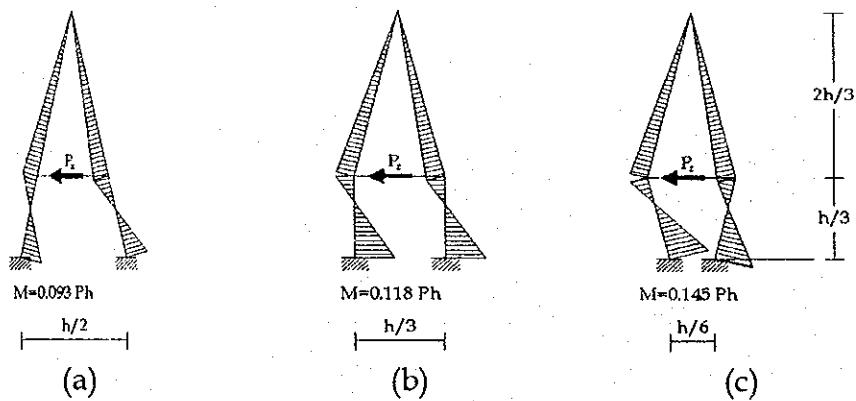
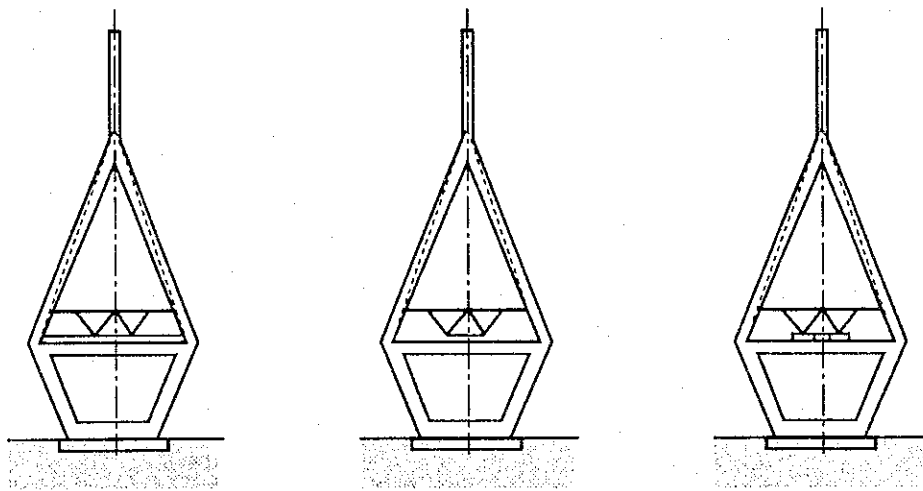


Figure 5.15 Bending Moment Diagram

(5) Supporting System

Normally, three supporting systems for the cable-stayed bridge can be considered. (a) Rigid Frame System is the simplest and best way to connect a girder and pier firmly with concrete. This connection, however, may be applied to a two-span cable-stayed bridge or for the flexible high piers. (b) The Floating System is effective by used for bridges where the horizontal force is smaller and restraint is not critical. (c) The Bearing Shoe System is a suitable solution a three span cable-stayed bridge with the bearing shoe system for the comparatively longer span length. It was recommended that option (c) Bearing Shoe System be adopted for the Can Tho Bridge.



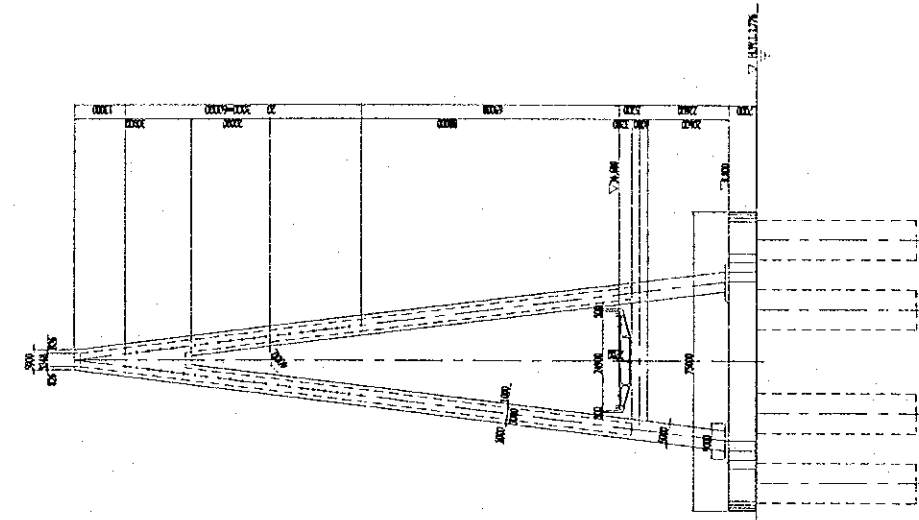
(a) Rigid Frame System (b) Floating System (c) Bearing shoe System

Figure 5.16 Supporting System

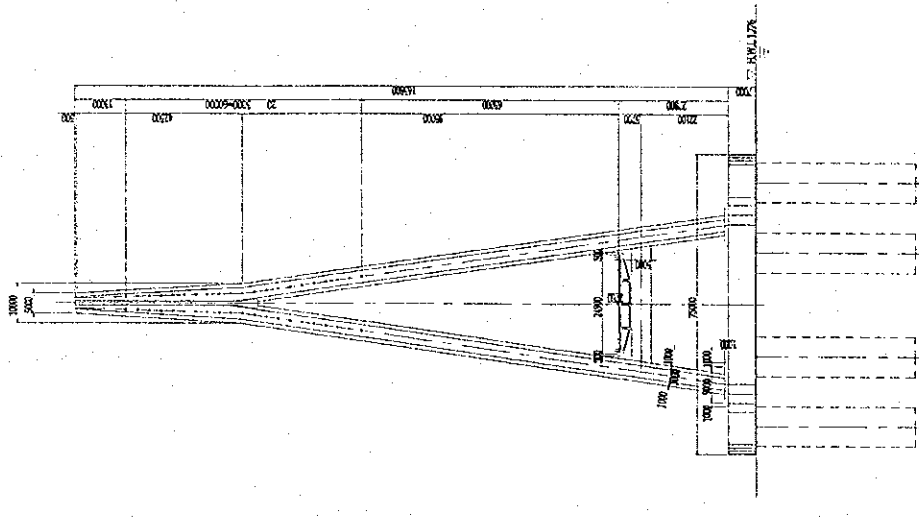
(6) Type of Substructure for the Main Bridge

The substructure type to be designed closely relates with the structural system of the superstructure, especially in the cases of cable bridge system. Normally, the cable bridge system requires higher towers. The crucial point for the tower of the Can Tho Bridge is that the projected height above the soil (which is to be the bearing stratum of the bridge foundations), is very large. The projected height will include the vertical navigational clearance, the river water depth and local scour depth around the bridge pier. Therefore, an ideal tower height should be as small as possible subject to the structural analysis of the bridge. Typical layouts of towers for each applicable type of main bridge are shown in Figure 5.17.

Alternative 3



Alternative 2



Alternative 1
(F/S)

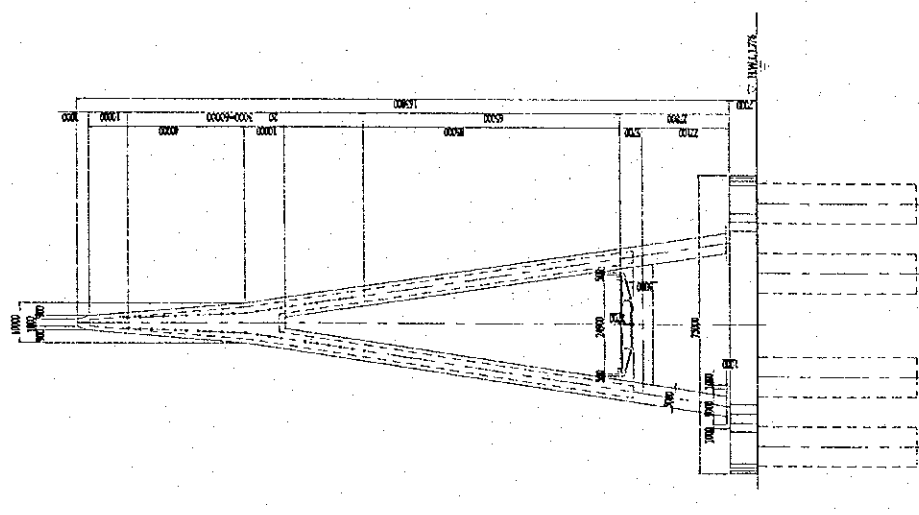
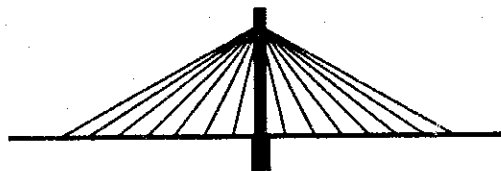


Figure 5.17 Layout of Main Tower

(7) Cable Arrangement

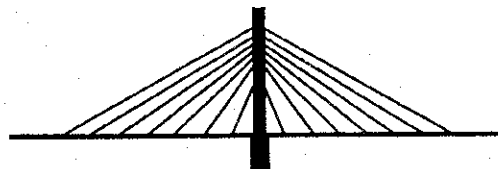
The cable arrangement of the cable-stayed bridge can be classified into three layouts.



Radial layout

Radial Layout

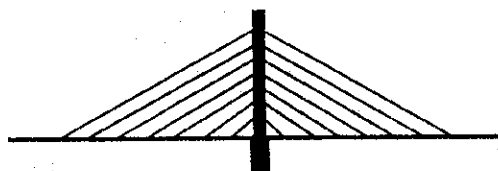
All the cables converge at the top of tower, so the anchors concentrate on a restricted section of the tower.



Fan layout

Fan Layout

The cables are regularly spread along the top part of the tower. It does not differ much from the radial layout but has the advantage of easier anchoring because the cables are further apart, and the cable angles are effective for the vertical lifting forces.



Harp layout

Harp Layout

The cables are parallel to each other and reduces the risk of tower instability, as the anchorage points are spread along the whole height of the tower. This allows simpler construction procedures, and is suitable for concrete tower construction.

Figure 5.18 Cable Arrangement

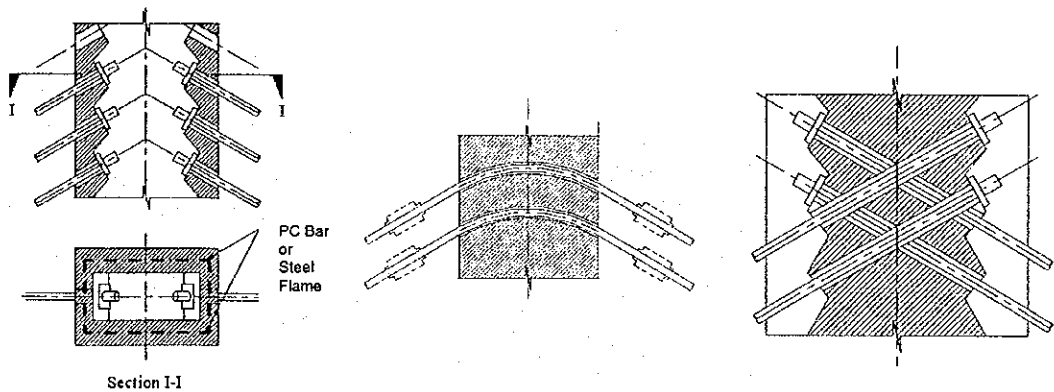
The Fan Layout is recommended because the effectiveness of cable angles to the main girder structure can be expected and the wider separation of the cable anchorages simplify the anchoring system.

(8) Anchorage System of Cables and Tower

The anchorage can be classified into three systems for the cable-stayed bridge.

- Inner Tower Anchorage
- Through Type Saddle
- Crossing Anchorage

The Inner Tower Anchorage is the recommended system as the anchorage is inside of the tower and can minimize corrosion. Ladders should be provided inside the tower for maintenance. The through Type Saddle system is not recommended due to the high cost of the large size and heavy steel structure of saddle which may cause high cost, and problems of material fatigue in the cable caused by repeated stress. The Crossing Anchorage system is also not recommendable due to the corrosion of anchorages exposed to the atmosphere, and torsion force which will be generated by differences of active force at each anchorage.



(a) Inner Tower Anchorage (b) Through type Saddle (c) Crossing Anchorage
 Figure 5.19 Anchorage System of Cables and Tower

(9) Connection of PC and Steel Girders

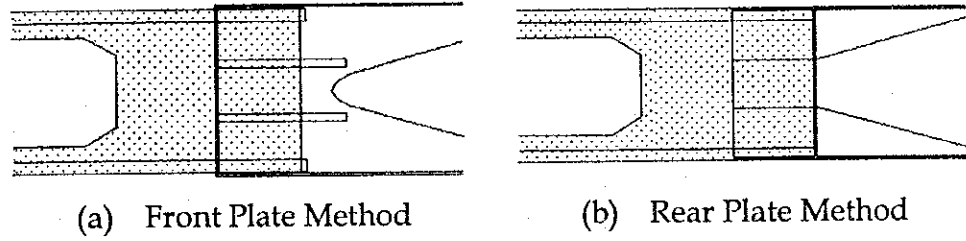
The geometrical moment of inertia between PC and steel girders is extremely different and the structural behaviors under dynamic loads are also quite different between them. Stress concentration occurs, and structural stress does not flow smoothly at the connection between PC and steel girders. This requires special detailed design for control of structural fatigue.

A solution is to provide a buffer zone which takes into consideration the difference of the rigidity between PC and steel girders. Basic consideration on the functions required for the connection systems are:

- Between PC and steel girders, the stress flow should be transferred smoothly.
- Rigidity of the girder section should not be changed abruptly.
- Easier and better construct ability should be maintained.

Normally, it is categorized into two systems, i.e. Overall Area Connection and Partial Area Connection as below:

a) Overall Area Connection



b) Partial Area Connection

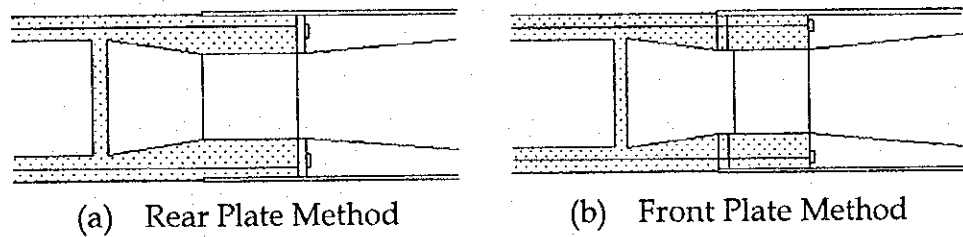


Figure 5.20 Connection System

The Partial Area connection is recommended because the rigidity at the connecting section is not changed abruptly, with the result that stresses flow smoothly. The schematic illustration is represented as below.

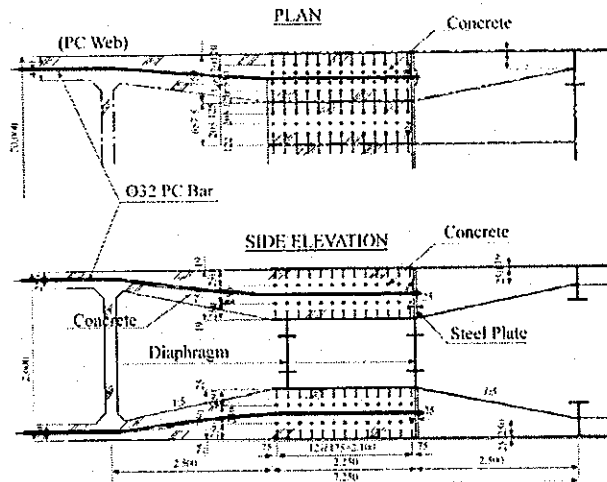


Figure 5.21 Connection Detail

5.3.7 Bridge Type and Span Arrangement for the Approach span Bridge

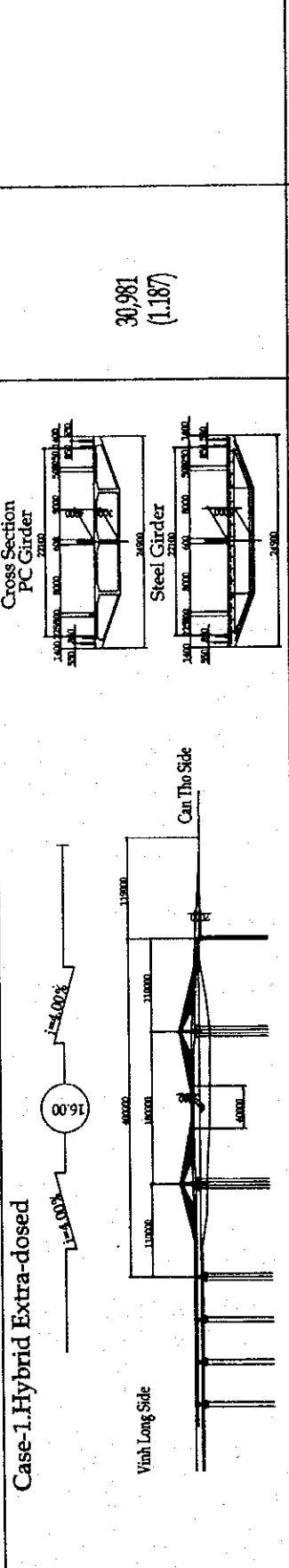
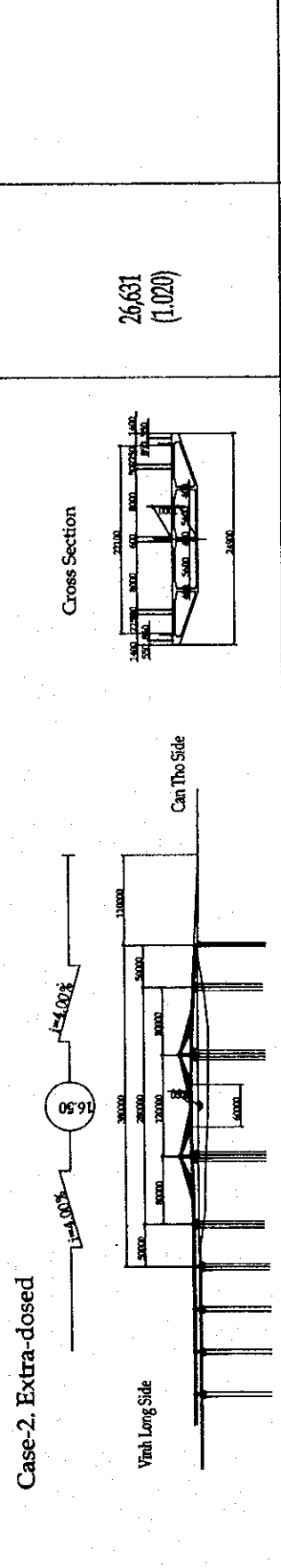
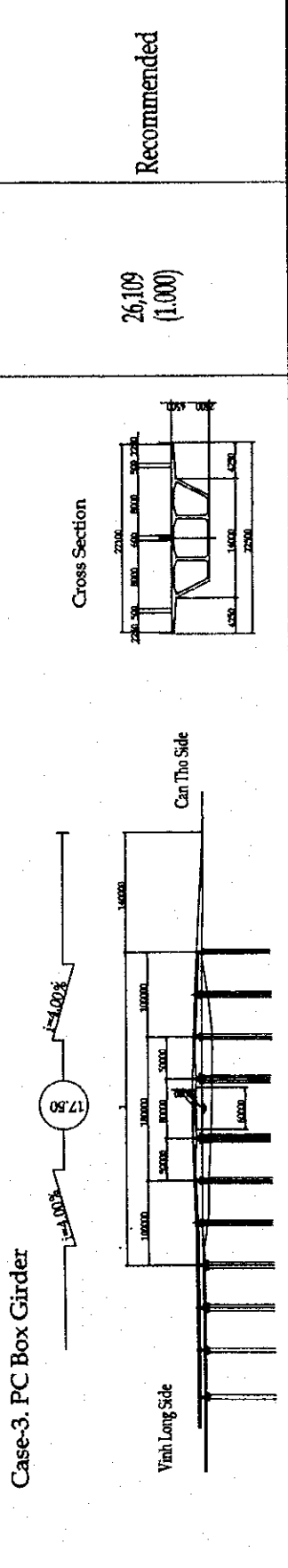
The appropriate bridge type and the optimum span length for the approach span bridges were determined in conjunction with the comparison of the

three bridge types for finding the most economical span length. For this study, a Continuous PC Composite Girder (40m), a Continuous PC Box Girder (50m), and a Continuous PC Box Girder (60m) were compared with each other on the basis of the construction cost of superstructure and substructure including foundations. The Continuous PC Composite Girder type (40m) was recommended, as it is the most viable economic alternative.

5.3.8 Bridge Type for the River Branch

In order to economize the bridge cost, the types of bridge crossing the river branch of the Hau River on the route were studied. The costs of the three applicable bridge types, Case-1 of a Hybrid Extra-dosed type with a central span length of 180.0m, Case-2 of a 120.0m span PC Extra-dosed type, and Case-3 of a 80.0m span PC box girder type were compared. The 9m vertical clearance and multiple 60m horizontal clearances (referring to the Technical Classification of Inland Waterways (TCVN-5664-1992), were consider for this comparison study as well as the deep soft subsoil conditions.

Compared with Case-2 of the PC Extra-dosed type, the Case-1 Hybrid type can achieve a longer central span using a steel structure but it is costly and the longer span length involves a more concentrated reaction transmitted from the superstructure to the soft ground, which creates an adverse situation. The Case-3 Box Girder type requires many piers due to the shorter spans involved. However, when compared with the Case-2 Extra-dosed Bridge, the cost difference is negligible. The Case-3 continuous PC Box Girder type has less technical problems compared with Case 1 and 2 and is more economically viable.

Configuration of Bridge and Gradient of Approach Portions	Cost \$1,000 (Ratio)	Remarks
<p>Case-1. Hybrid Extra-dosed</p> 	<p>30,981 (1.187)</p>	
<p>Case-2. Extra-dosed</p> 	<p>26,631 (1.020)</p>	
<p>Case-3. PC Box Girder</p> 	<p>26,109 (1.000)</p>	<p>Recommended</p>
<p>THE DETAILED DESIGN OF THE CAN THO BRIDGE CONSTRUCTION IN SOCIALIST REPUBLIC OF VIET NAM</p>		<p>Figure 5.22 Study on Bridge Types for the River Branch JAPAN INTERNATIONAL COOPERATION AGENCY</p>

5.3.9 Bridge Type and Applicable Span Length of the Bridges for the Approach Road Sections

The bridge types to be design for the approach road section should cover the following conditions: reduced construction time, ease of construction, good quality control, and to minimize concrete creep and shrinkage, etc. From these viewpoints, the relationship between bridge type and applicable span length are shown as below:

Table 5.7 Bridge Type and Applicable Span Length (Approach Road Section)

TYPE OF GIRDER	SPAN LENGTH (m)						
	10	15	20	30	40	50	60
RC HOLLOW SLAB *1 (JAPAN)	10	15					
PC-T (PRE-TENSION) (VIETNAM)	10	15					
PC-T (POST-TENSION) (VIETNAM)		15	20	30			
PC-I (POST-TENSION) (US,AASHTO)			20	35	40		
PRC-Hollow *1 :20 ~ 35m (JAPAN)			20	35	40		
PC-BOX (JAPAN)				35		50	60
PC-BOX (JAPAN) (BALANCED CANTI LEVER)						50	60~150

Note : ※ 1For road embankment or rampway of interchange

5.3.10 Selection of Foundation Type for the Tower Pier of the Main Bridge

The possible types for the foundation of the main tower are the following four types i.e., Steel Pile Sheet Pile, Cast-in-situ Wall, Multi Columns Open Caisson Foundation and Cast-in-situ Pile in consideration of severe natural conditions such as hydrodynamic (local scouring around the pier), deep bearing stratum, construction method, and construction cost.

(1) Steel Pile Sheet Pile

Possible penetration is 80m, so it can not reach to the depth required for bearing capacity. If with 80m deep and wider foundation, it still can not solve the displacement control which affect to the superstructure.

(2) Cast-in-situ Wall

The penetration depth can reach to the possible bearing stratum (120m deep). The problems of this method are hydrodynamic problem

against the flow velocity and higher construction costs including the preparation of the staging and equipment.

(3) Open Caisson Foundation

Structurally, it is desirable type, especially the control of structural influence to the superstructure. However, it requires higher construction costs including special jacking set and sophisticated sinking caisson operation.

(4) Cast in Place Pile

The penetration depth can reach to the possible bearing stratum. However, to hold the necessary rigidity (moment of inertia) to control the influence to the superstructure, it requires greater number of piles which appears above the riverbed.

Among the four types, open caisson foundation and cast in place pile are the most possible type from the technical and economical reasons. Table 5.8 shows further comparison of them.

Table 5.8 Comparison of Foundation for the Tower Pier of the Main Bridge

Description	Open Caisson ($\phi 10.0\text{m}$)	Cast in Place Pile ($\phi 3.0\text{m}$)
Construction Cost	Δ	\circ
Construction of Extremely Deep Foundation (100m)	Δ	\circ
Influence to Superstructure (Rigidity: Moment of Inertia)	\circ	Δ^*
Duration of Construction Period	Δ	Δ
Quality Control (Concrete)	\circ	Δ
Quality Control (Drilling/Excavation)	Δ	\circ
Hydrodynamic Problem	Δ^{**}	Δ
Confirmation of Bearing Capacity	Δ	\circ

Note:

\circ : Fair

Δ : Comparatively Problem

* : To consider steel casing of pile

** : Simulation analysis was conducted

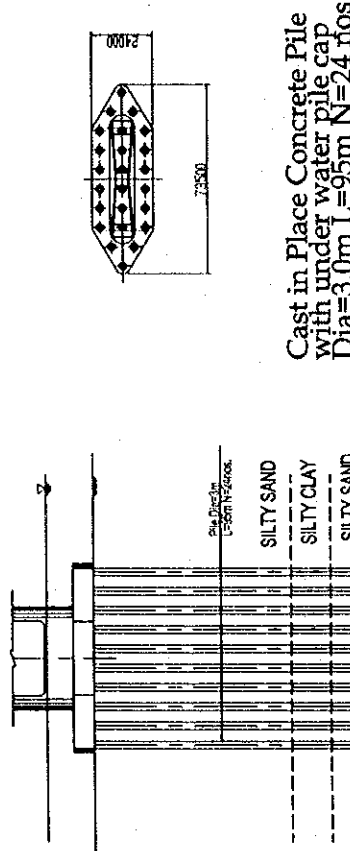
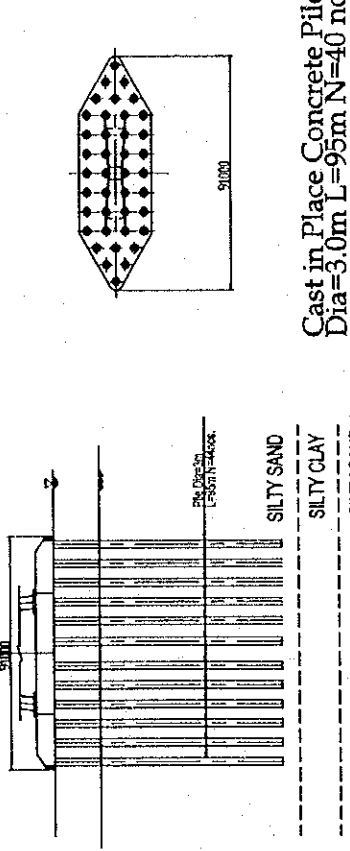
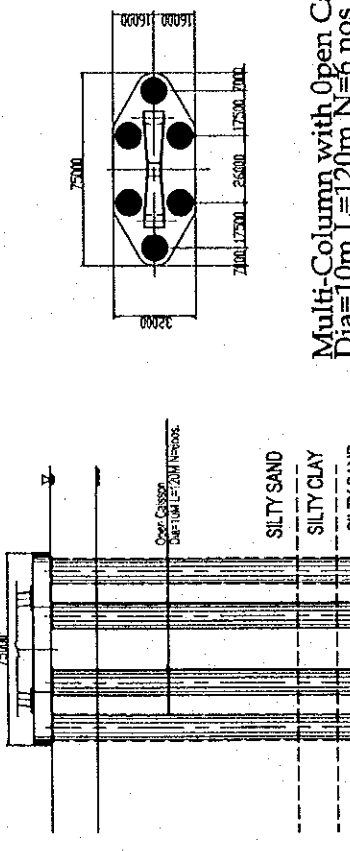
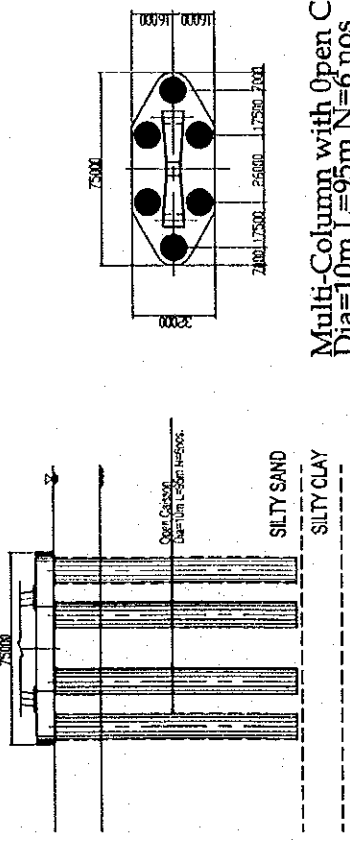
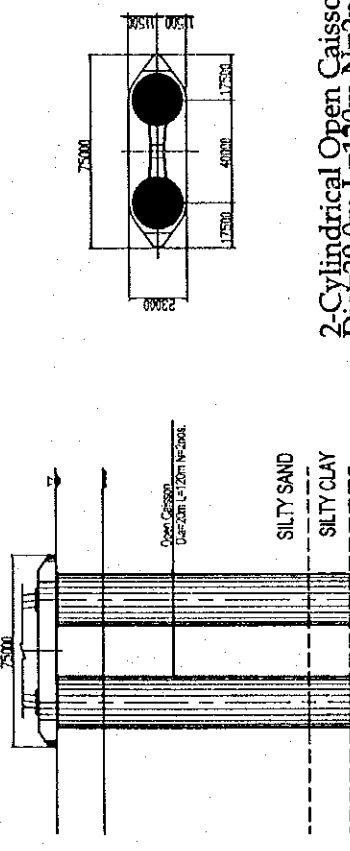
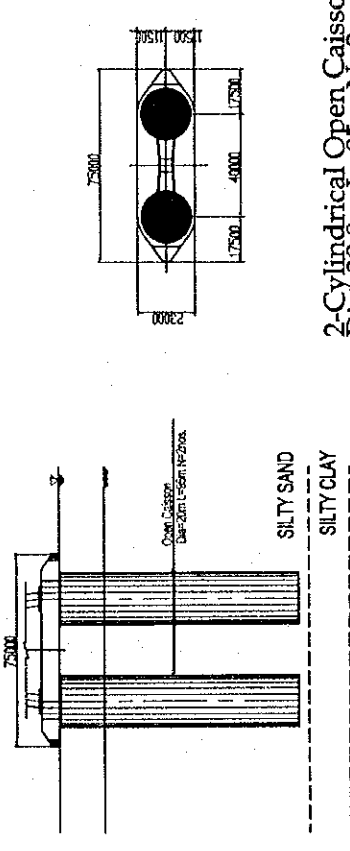
5.3.11 Further Comparison of Foundation Types of Open Caisson and Cast in Place Pile

Comparison studies were carried out for the foundation types for suitability from the technical and economical viewpoints. From the results of boring logs and soil profile, it was recognized that there is a silty clay layer at the depth of 100 to 125m below the water level, and soils above and below this silty clay were fine sand. Therefore, two levels of bearing stratum were available for support the foundation, and were considered for comparison of types. The following six cases were studied.

- Cast-in-place Pile (under water pile cap) : ϕ 3.0m x 100m, 24 nos.
- Cast-in-place Pile : ϕ 3.0m x 95m, 40 nos.
- Multi-column with Open Caisson : ϕ 10.0m x 120m, 6 nos.
- Multi-column with Open Caisson : ϕ 10.0m x 95m, 6 nos.
- 2-Cylindrical Open Caisson : ϕ 20.0m x 120m, 2 nos.
- 2-Cylindrical Open Caisson : ϕ 20.0m x 95m, 2 nos.

Finally, Cast-in-place Concrete Pile was concluded for the foundation type of the tower pier of the Main Bridge from the technical and economical reasons.

COMPARISON OF FOUNDATION TYPE FOR MAIN TOWER(MAIN BRIDGE)

Foundation Type	Configuration of Foundation	Descriptions
Alternative 1 Cast in Place Concrete Pile with under water pile cap Dia=3.0m L=100m N=30nos.		Structural Features (1) The pile length is shorter. (2) More stiffness can be expected compared to the outstanding types. (3) Large scale temporary works are required due to execution of pile cap works. Construction Period 23 months/pier Construction Cost(Ratio) 1.061 Evaluation Stability: ○ Quality Control: △ Const.-Cost: △ Const.-Period: △ Local Scouring: △
Alternative 2 Cast in Place Concrete Pile Dia=3.0m L=95m N=40nos.		Structural Features (1) The piles penetrate stratum of the sand above silty clay. (2) The displacement becomes large although the length of the pile become shorter. (3) The number of pile is increased. (4) There is problem in the stiffness of piles due to longer outstanding. Construction Period 26 months/pier Construction Cost(Ratio) 1.000 Evaluation Stability: △ Quality Control: △ Const.-Cost: △ Const.-Period: ○ Local Scouring: △
Alternative 3 Multi-Column With Open Caisson Dia=10.0m L=120m N=6nos.		Structural Features (1) Due to the water depth, the fist block of caisson is steel-shell. (2) Special excavator and hydraulic jacks be used for caisson sinking. (3) Rigidity of foundation can be maintained. Construction Period 28 months/pier Construction Cost(Ratio) 1.000 Evaluation Stability: ○ Quality Control: ○ Const.-Cost: △ Const.-Period: △ Local Scouring: △
Alternative 4 Multi-Column With Open Caisson Dia=10.0m L=95m N=6nos.		Structural Features (1) The construction method is the same as avobe plan. (2) The caisson bottom is to be penetrated to the sand layer below silty clay. Construction Period 25 months/pier Construction Cost(Ratio) 0.973 Evaluation Stability: △ Quality Control: ○ Const.-Cost: ○ Const.-Period: ○ Local Scouring: △
Alternative 5 2-Cylindrical Open Caisson Dia=20.0m L=120m N=2nos.		Structural Features (1) 2-large size cylindrical open-caisson are provided the transverse direction. (2) Due to the large size of caisson, the heavy and large equipment are required. Construction Period 26 months/pier Construction Cost(Ratio) 1.100 Evaluation Stability: ○ Quality Control: ○ Const.-Cost: △ Const.-Period: ○ Local Scouring: △
Alternative 6 2-Cylindrical Open Caisson Dia=20.0m L=95m N=2nos.		Structural Features (1) The construction method is the same as avobe type. (2) The caisson bottom is to be penetrated the sand layer above silty clay. Construction Period 22 months/pier Construction Cost(Ratio) 1.030 Evaluation Stability: △ Quality Control: ○ Const.-Cost: △ Const.-Period: ○ Local Scouring: △
THE DETAILED DESIGN OF THE CAN THO BRIDGE CONSTRUCTION IN SOCIALIST REPUBLIC OF VIET NAM		Figure 5.23 Comparison of Foundation Types (Main Bridge)
		JAPAN INTERNATIONAL COOPERATION AGENCY

Chapter 6

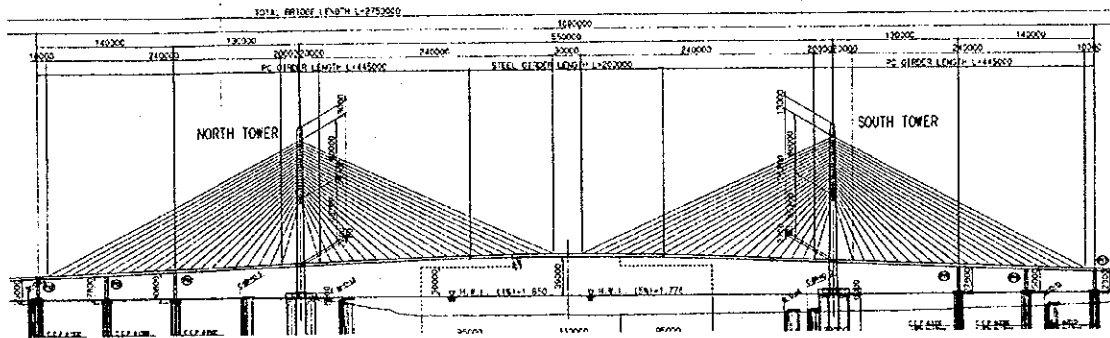
WIND TUNNEL TEST

CHAPTER 6 WIND TUNNEL TEST

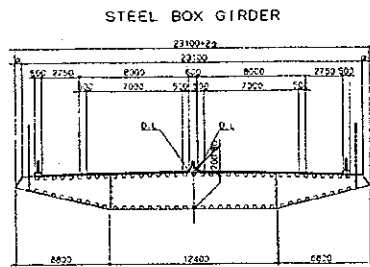
6.1 General Description of Can Tho Bridge

The Can Tho Bridge is planned to cross the Hau River in the city of Can Tho and to function as a by-pass of the National Highway Route 1. The bridge will be a steel-concrete composite cable-stayed bridge with a center span length of 550 m and a total length of 1,090 m.

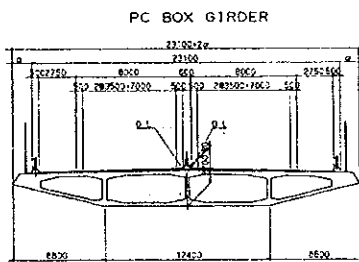
General plans are shown in Figure 6.1.



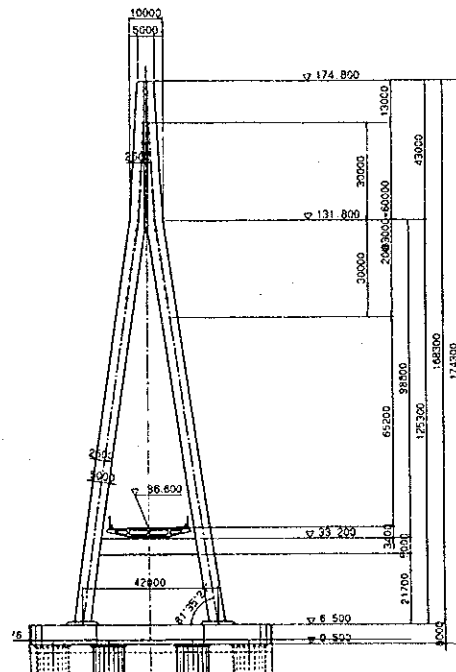
(Front View)



(Steel Section)



(Concrete Section)



(Tower)

Figure 6.1 General Plan of Can Tho Bridge

The possible center span length of cable-stayed bridges has extended recently. The longest-span bridge is the Tataru Bridge (890 m) in Japan

followed by the Normandie Bridge (856 m) in France. Next are the Yanpu Bridge (602 m) in China and the Central Meiko Bridge (590 m) in Japan.

The Can Tho Bridge is in the same center span length range as these last two. Thus, at this center span length, a careful investigation of aerodynamic stability is required.

6.1.1 Dimensions of Bridge

Dimensions of the bridge are shown below.

Type	3-span continuous cable-stayed bridge Deck: steel-concrete composite (steel: 200-m-long portion in center span) Tower: concrete
Length	1,090 m in total 550 m in center span
Deck	Box girder 2.7 m in height
Tower	Inverse Y shape 168.3 m in height
Cable	Twin cable planes 8 × 21 = 168 cables

6.2 Methodology of Wind Tunnel Testing

6.2.1 Aeroelastic Phenomena of Long-Span Bridge

Aeroelastic phenomena of long-span bridges are classified into several categories considering design. Wind-resistant-design code [2.1] of the Honshu-Shikoku Bridge Authority classifies them as shown in Figure 6.2.

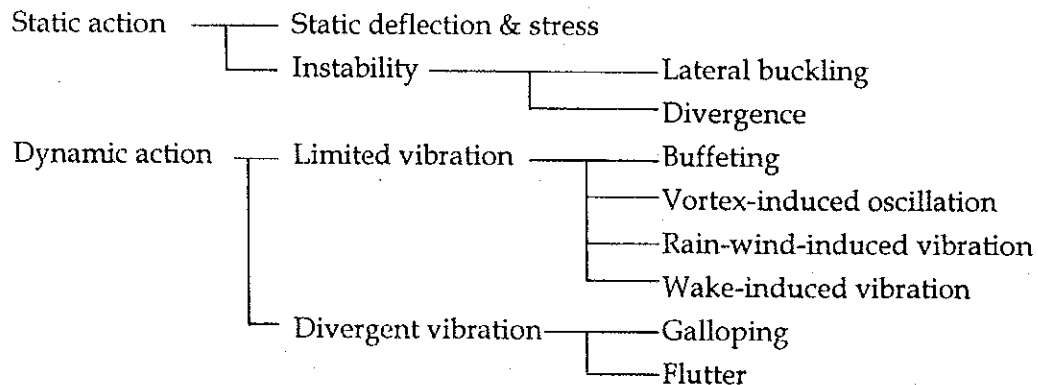


Figure 6.2 Classification of Aeroelastic Phenomena of Long-Span Bridges [2.1]

Static deflection & stress are stationary phenomena which are independent of time. They are caused by a mean component of time-varying wind speed.

Lateral buckling is typically observed at a very slender deck of a suspension bridge, which suddenly buckles normal to wind axis. The critical wind speed of occurrence is usually higher than that of flutter and galloping. Divergence is a phenomenon that a torsionally weak deck suddenly twists at a critical wind speed.

Limited vibrations are defined to be limited in terms of limited amplitude and/or limited wind-speed range. Buffeting is a random vibration due to turbulence in wind flow. It is usually estimated by a numerical analysis and is associated with an estimation of the maximum wind load. Vortex-induced oscillation is caused by well-known Karman Vortices formed on the leeward side of the structure. Since it is not a catastrophic phenomenon, it is viewed as harmful problem to the serviceability such as fatigue and discomfort to users. Rain-wind-induced vibration is often observed at stay cables of a cable-stayed bridge with the condition of wind and raining. The cause of the vibration is due to the formation of a water rivulet on the cable surface and the existence of the axial flow on the leeward surface, both are typical phenomena on an inclined cable. Wake-induced vibration is observed at the leeward structure of parallel-aligned structures such as twin cables and twin decks.

Divergent vibrations are catastrophic once they occur. They must not occur in the design wind-speed range. Galloping, which is vibration with a vertically dominant component, is typically observed at cables and bluff decks where lift coefficients show a negative slope. Flutter is often classified into "torsional flutter" and "bending-torsion flutter (or coupled flutter)" based on the vibration mode. The well-known collapse of the old Tacoma Narrows Bridge was caused by flutter.

6.2.2 Wind-Resistant Design for Long-Span Bridges

Wind-resistant design of bridges is done by a designer estimating how a bridge responds to wind flows and judging whether the responses are allowable or not. Furthermore, if the response exceeds a limit, appropriate countermeasures are required such as change of geometry of the bridge and/or attachment of stabilizing devices.

The key to successful and accurate wind-resistant design really depends on the accurate estimation of aerostatic/dynamic forces exerting on the bridge structure and of bridge responses. Since the bridge geometry is too complex to analyze flow patterns around it, wind-tunnel testing is the most reliable and reasonable method to execute wind-resistant design.

6.2.3 Methodology of Wind-Tunnel Testing

Types of Tests [2.2]

There are several kinds of wind-tunnel testing, each of which has a different purpose, as shown in Table 6.1.

Aerostatic-force coefficients, which are a function of angle of attack, are used to estimate wind load and buffeting responses. On the other hand, unsteady aerodynamic force coefficients (flutter derivatives), which are motion dependent, are sometimes measured with a section model. The flutter derivatives govern the state (damping & stiffness) of the bridge in wind flow and are used to numerically estimate flutter and/or buffeting.

The spring-mounted model test has widely been carried out to investigate the aerodynamic characteristics of the bridge deck because the test is relatively easy and inexpensive. The test assumes two dimensions structurally and aeroelastically, that is, the same dimensions of the deck cross section along the bridge span and a small torsional deflection of the deck due to wind loading.

For the purpose of investigating the three dimensional effects, the taut strip model test and/or full-model test are sometimes carried out, which are relatively time-consuming and expensive, however. In particular, the full-model test needs a very careful modeling and preparation. However, once the test is executed, it has a big advantage for one to directly evaluate the aerodynamic responses of the full-scale bridge. Both of the two testing methods also have an advantage that they can include the effects of the boundary layer turbulence.

Table 6.1 Types of Wind-Tunnel Testing

Name of tests	Quantities measured	Model used	Output	Model scale
Static-force measurement test	Aerostatic force coefficients (C_D, C_L & C_M)	Rigid section model	Coefficients (C_D, C_L & C_M) - angle of attack	1/50 - 1/100
Spring-mounted model test (section model test)	Dynamic & static deflection Aerodynamic damping	Rigid section model	Deflection (amplitude) - wind speed	1/50 - 1/100
Taut strip model test		3D partial-bridge model	Aerodynamic damping - wind speed	1/100 - 1/300
Full-model test		Elastic full model		1/70 - 1/300

Similarity Law [2.2 & 2.3]

Executing wind-tunnel testing, several similarity requirements are imposed. They are:

- (1) Inertia parameter: ρ_s/ρ
- (2) Elastic parameter: $E/(\rho U^2)$
- (3) Gravity parameter (Froude number): gD/U^2
- (4) Viscous parameter (Reynolds number): UD/ν
- (5) Damping parameter: δ_s

where ρ : air density, ρ_s : density of the structure, E : Young modulus, U : wind speed, ν : kinematic molecular viscosity of the fluid, D : representative length.

The viscous parameter is difficult to satisfy, so the remaining four parameters are usually considered.

Since the third parameter (Froude number) affects a gravity-governing structure such as a suspension bridge cable, the testing for a section model of a bridge deck and an elastic tower model can neglect this parameter. After all, three parameters (inertia, elasticity, and damping) are required to satisfy in this research.

6.3 Section Model Test of Deck

6.3.1 Description of Test

The aerodynamic stability (characteristics) of the bridge completed was investigated by a section model test, as shown in Figures 6.3 and 6.4. As described in Chapter 2, the section model of the deck is mounted by 4 springs at each side. The model is given two degree-of-freedom (vertical and torsion) and the similarity requirements are satisfied.

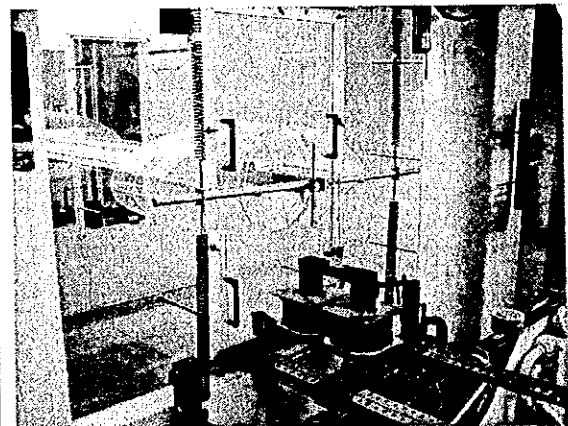
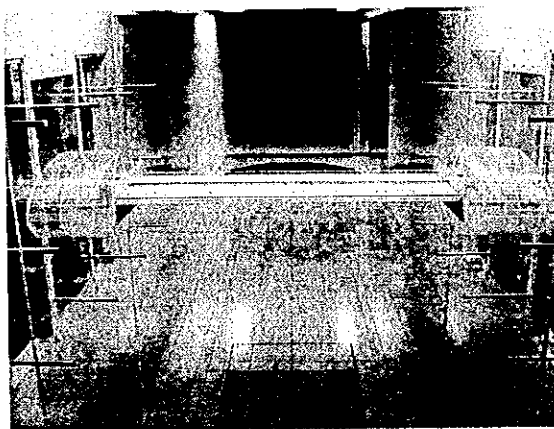


Figure 6.3 Section Model of Deck

Figure 6.4 Spring-Mount System

The similarity requirements in the section model are

- (1) Inertia parameter: $m/(\rho D^2), I_p/(\rho D^4),$
- (2) Elastic parameter: $U/(f_h D), U/(f_\theta D)$
- (3) Damping parameter: $\delta_{s, h}, \delta_{s, \theta},$

where m : equivalent mass, I_p : equivalent polar moment of inertia, ρ : air density, D : length, U : wind speed, f : frequency, δ_s : structural damping. The subscripts of h and θ represent vertical and torsion, respectively.

The inertia parameters were adjusted by putting additional masses at appropriate positions so as to satisfy the parameter. The elastic parameters (frequency parameter) were adjusted by spring stiffness and the distance of two springs. The damping parameters were adjusted by using electrical damping devices as shown in Figure 6.4.

In the test, aerodynamic responses were measured with changing wind speed. A smooth flow was used in the test.

The scale of the section model is 1/60 and its length 1.25 m. Test conditions are shown in Table 6.2. The frequency ratio of vertical and torsion is by 11 % lower than requirement. Since the ratio affects the flutter onset speed, flutter onset speed if measured can be converted with the Selberg formula. In addition, since vertical and torsional vortex-induced oscillation are one degree-of-freedom, the difference of the frequency ratio can be dissolved by applying different wind-speed ratio between vertical and torsion.

Table 6.2 Test Conditions

	Prototype	Requirement in test	Measured in test	Error (%)
Equivalent mass m (kgf/m)	33.11×10^3	9.197	9.085	- 1.2
Equivalent polar moment of inertia I_p (kgf·m ² /m)	2231.2×10^3	0.1722	0.1697	- 1.5
Vertical frequency f_h (Hz)	0.395	-	1.66	-
Torsional frequency f_θ (Hz)	1.230	-	4.59	-
Frequency ratio (f_θ/f_h)	3.11	3.11	2.77	- 10.9
Structural damping	-	0.02	0.02	0
Vertical: $\delta_{s, h}$	-	0.02	0.02	0
Torsion: $\delta_{s, \theta}$	-	0.02	0.02	0

The ratio of wind speed between model and full-scale is given by

$$\frac{f_p B_p}{U_p} = \frac{f_m B_m}{U_m} \quad (4.1)$$

where subscripts p and m represent full-scale (prototype) and model, respectively. Based on the conditions in Table 6.2, the wind-speed ratios of vertical and torsion are 11.9 and 13.4, respectively.

As for structural damping, it tends to show the trend that damping decreases as the span length increases. Based on previous research, structural damping for vertical and torsion was assumed to be 0.02 in log decrement. Responses with the damping of 0.03 were also investigated, however.

Three angles of attack of wind flow were chosen, that is, -3 degrees, 0 degree, and +3 degrees.

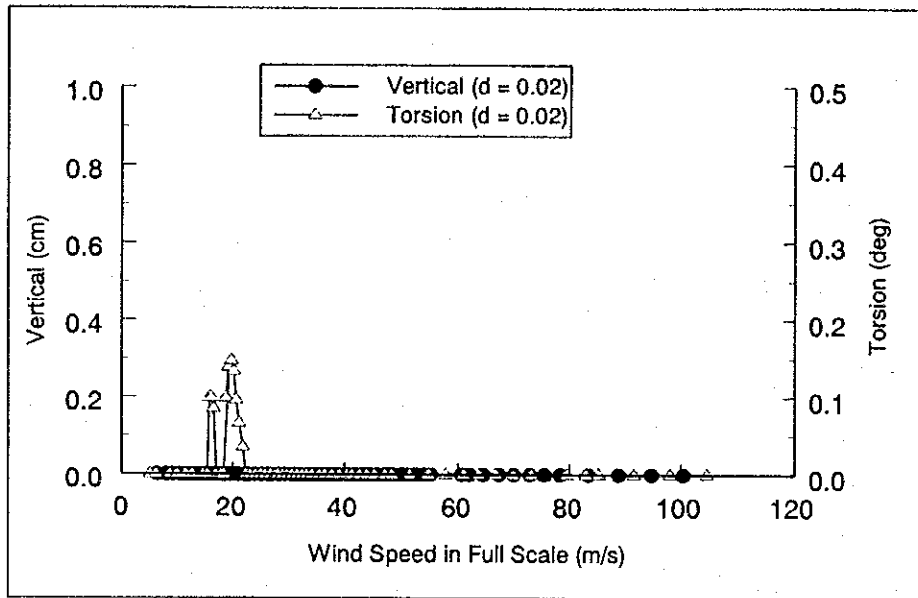
6.3.2 Test Results

The test results (V - A diagrams), which are vertical and torsional responses versus wind speed, are shown in Figures 6.5 - 6.7. The vertical and horizontal axes are converted to the dimensions in the full-scale bridge.

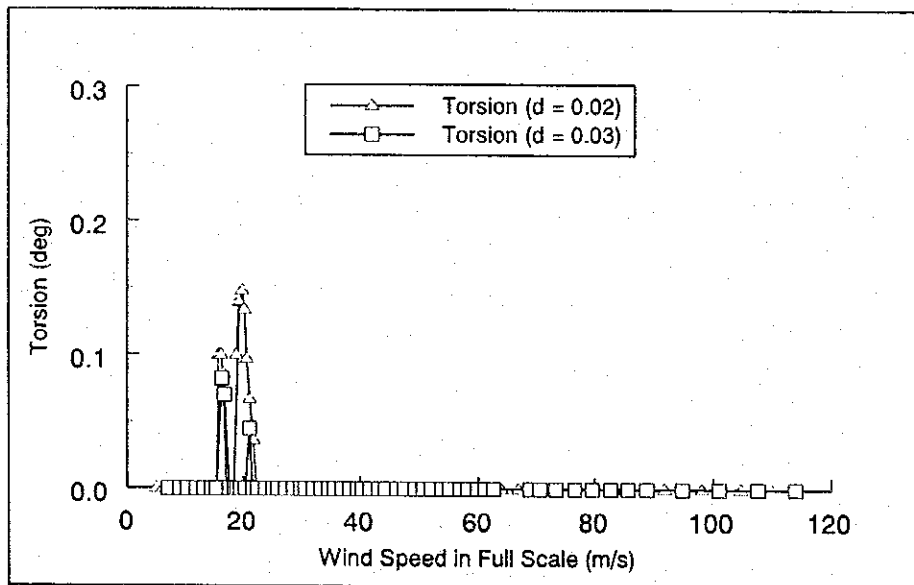
In the case of angle of attack being 0 degree, it was observed that torsional vortex-induced oscillation with amplitude of 0.15 degree would occur at a wind speed of about 20 m/s. However, increasing the structural damping from 0.02 to 0.03 in log decrement suppressed the amplitude to about 0.08 degrees. No vertical vibration was observed. As for flutter, it would not occur until a wind speed of 100 m/s. Coupled flutter was observed to occur at about 311 m/s, however.

In the case of angle of attack being + 3 degree, it was observed that torsional vortex-induced oscillation would occur at a wind speed of about 15 m/s as observed in 0 degree. However, the amplitude was relatively small and about 0.04 degrees. Increasing the structural damping to 0.03 in log decrement completely suppressed the vibration. No vertical vibration was observed. As for flutter, it would not occur until a wind speed of 320 m/s which was the maximum wind speed of the test.

In the case of angle of attack being - 3 degree, relatively small-amplitude (about 0.04 degrees) torsional vortex-induced vibration was observed. On the other hand, vertical vortex-induced vibration with amplitude of about 2.9 cm was observed at a wind speed of 9 m/s. Increasing the structural damping to 0.03 in log decrement completely suppressed the torsional vibration, but slightly suppressed the vertical to about 2.5 cm. As for flutter, coupled flutter was observed at a wind speed of 281 m/s.



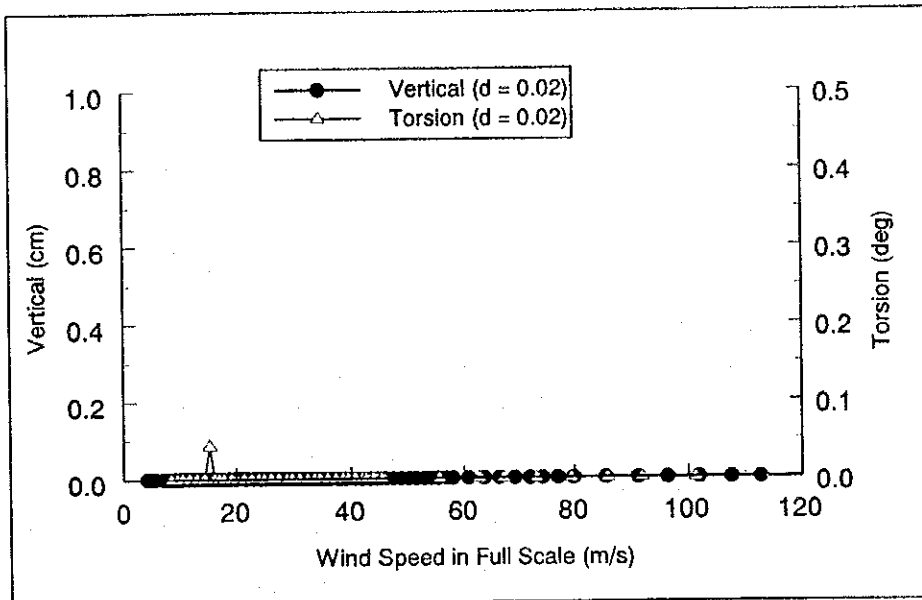
(1) Vertical & Torsion ($d = 0.02$)



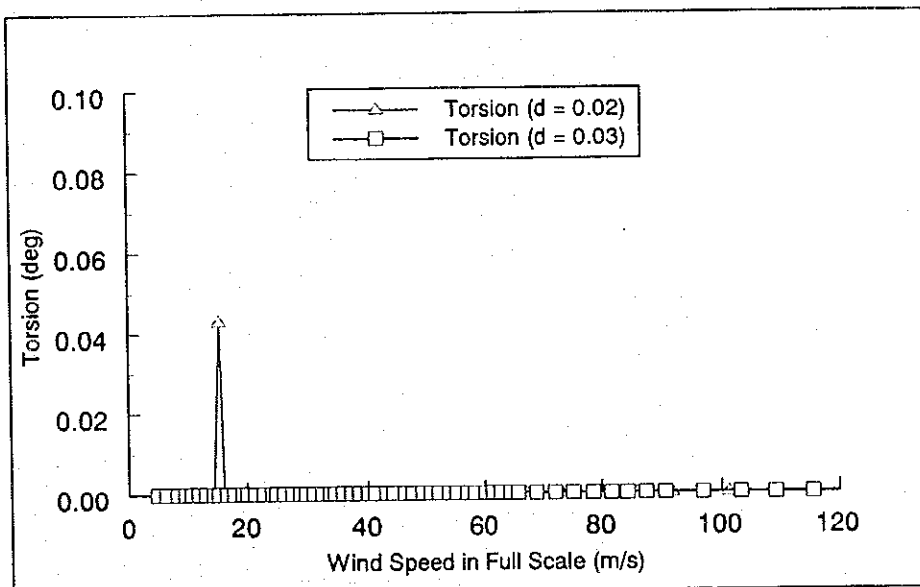
(2) Torsion ($d = 0.02$ & 0.03)

Relationship between Responses and Wind Speed ($\alpha = 0$ deg)

Figure 6.5 Relationship between Vertical & Torsional Responses and Wind Speed (angle of attack = 0 degree)



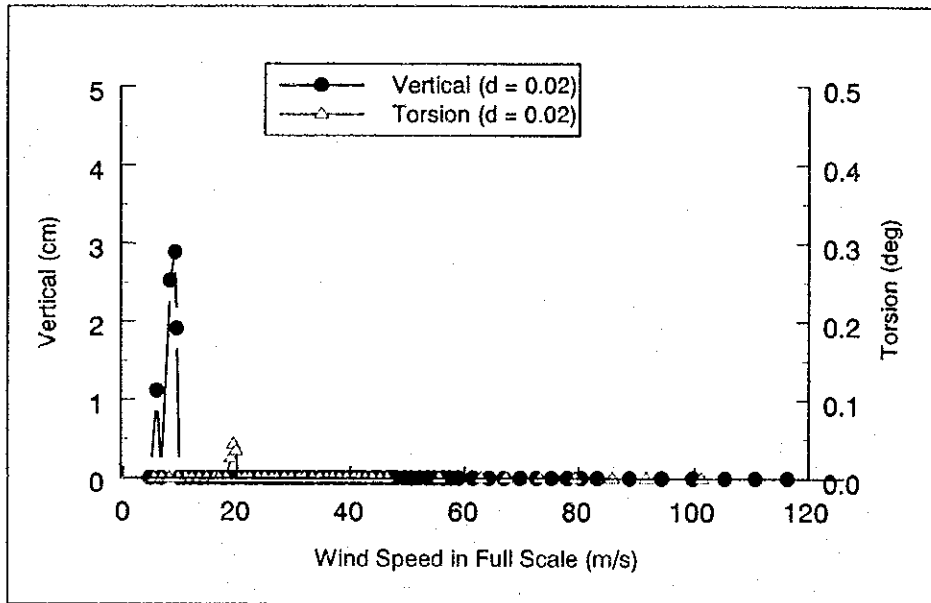
(1) Vertical & Torsion ($d = 0.02$)



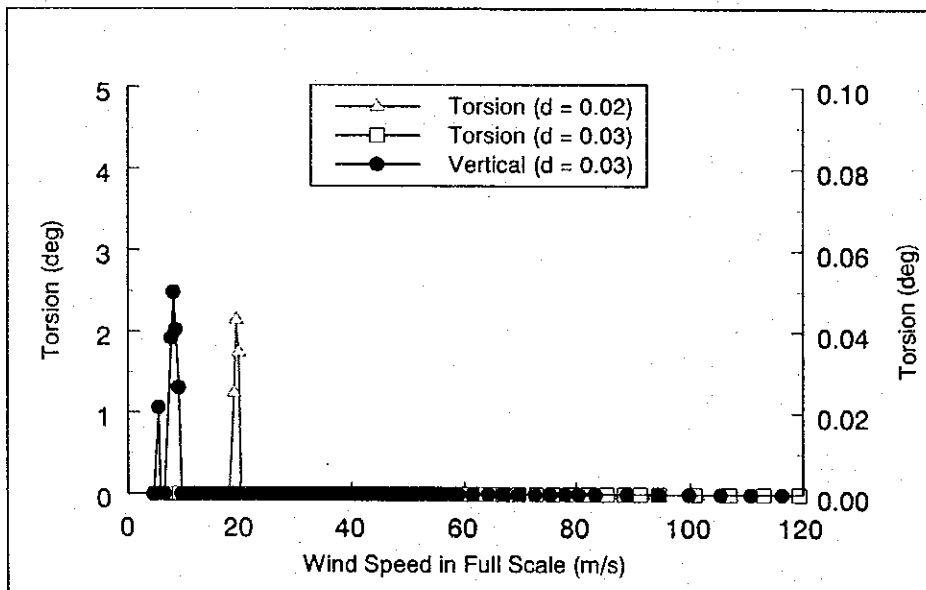
(2) Torsion ($d = 0.02$ & 0.03)

Relationship between Responses and Wind Speed ($d = +3$ deg)

Figure 6.6 Relationship between Vertical & Torsional Responses and Wind Speed (angle of attack = +3 degrees)



(1) Vertical & Torsion ($d = 0.02$)



(2) Vertical & Torsion ($d = 0.02$ & 0.03)

Relationship between Responses and Wind Speed ($d = -3$ deg)

Figure 6.7 Relationship between Vertical & Torsional Responses and Wind Speed (angle of attack = -3 degrees)

6.3.3 Judgment of Aerodynamic Stability of Deck

The reference wind speed at 10 m, U_{10} is specified as 40 m/s for the Can Tho Bridge. Based on U_{10} , the design wind speed for the deck is calculated as follows [2.1 & 4.1]:

The reference height of the deck is given as the average of shear center height at tower location (36 m) and that at the span center (43 m), that is, 40 m (= [36 + 43] / 2).

Assuming the power law for wind-speed profile and the power of 0.16 (ground roughness category: II), the design wind speed for the deck of the Can Tho Bridge is calculated as

$$U_D = 40 \times \left(\frac{40}{10}\right)^{0.16} = 50 \text{ m/s} \quad (4.1)$$

The verification wind speed for vortex-induced vibration is defined to be the same as the design wind speed, which is 50 m/s.

The flutter verification wind speed is defined as follows:

$$U_{vf} = 1.2 \times E_{r1} \cdot U_D = 1.2 \times 1.15 \times 50 = 69 \text{ m/s} \quad (4.2)$$

where E_{r1} : modification factor for wind-speed fluctuations and 1.2: safety factor.

As for vortex-induced vibration, it is primarily required that any vibration would not occur below the verification wind speed. If it occurs, the amplitude of the vibration must be less than an allowable limit. The limit is defined in terms of structural strength, fatigue and discomfort for users.

The wind-resistant design manual for road bridges [4.1] specifies the limit as follows:

[Vertical vortex-induced vibration]

$$h_a = 0.04/f_h = 0.04/0.395 = 0.101 \text{ m} \quad (4.3)$$

[Torsional vortex-induced vibration]

$$\theta_a = 2.28/(bf_\theta) = 2.28/(9.68 \times 1.23) = 0.19 \text{ deg} \quad (4.4)$$

where f_h and f_θ : natural frequencies of vertical and torsion, b : distance between deck center and pedestrian lane (= 9.68 m).

Referring to the specified values above, the judgment of the aerodynamic stability of the deck of the Can Tho Bridge is made below and shown in Tables 6.3 and 6.4.

As for flutter, flutter wind speeds measured in all cases are far beyond the verification wind speed. This will lead to the conclusion that the bridge is stable for flutter.

As for vortex-induced vibration, the vibration amplitude even in case of the structural damping being 0.02 in log decrement is less than the allowable limit. This will conclude that the vortex-induced vibration would not cause my problem.

Table 6.3 Judgment for Flutter

Angle of attack	Flutter speed measured	Flutter speed modified *)	Flutter verification wind speed
0 degree	311 m/s	354 m/s	
+ 3 degree	> 320 m/s	> 365 m/s	69 m/s
- 3 degree	281 m/s	320.6 m/s	

*) Flutter speed measured was modified by Selberg Formula ($\times 1.14$).

Table 6.4 Judgment for Vortex-Induced Vibration

Angle of attack	Vertical vortex-induced vibration		Torsional vortex-induced vibration	
	max. amplitude measured	allowance	max. amplitude measured	allowance
0 degree	-		0.15 deg	
+ 3 degree	-	10.1 cm	0.04 deg	0.19 deg
- 3 degree	2.9 cm		0.04 deg	

*) Amplitude measured is based on structural damping of 0.02 in log decrement.

[Selberg Formula]

In this test, the frequency ratio between vertical and torsion, which affects the flutter wind speed, is by 11 % lower than the requirement. Although the flutter wind speeds measured were far greater than the verification, the flutter speeds measured were modified by the Selberg Formula.

$$U_{cf} = 0.44 \times (2\pi f_0) \times B \sqrt{\left(1 - \left(\frac{f_h}{f_0}\right)^2\right) \frac{\sqrt{v}}{\mu}} \quad (4.5)$$

where $v = \frac{8I_p}{mB^2}$ and $\mu = \frac{\pi\rho B^2}{2m}$.

Based on the values in Table 4.1 and using the Selberg Formula (Eq. (4.5)),

the ratio of flutter wind speeds between 3.11 and 2.77 in frequency ratio is calculated as

$$\frac{U_{cf}}{U_{cf}'} = \frac{f_0}{f_0'} \sqrt{\frac{1 - \left(\frac{f_h}{f_0}\right)^2}{1 - \left(\frac{f_h}{f_0'}\right)^2}} = \frac{0.395 \times 3.11}{0.395 \times 2.77} \sqrt{\frac{1 - (1/3.11)^2}{1 - (1/2.77)^2}} = 1.14 \quad (4.6)$$

where (') represent values in the frequency ratio of 2.77.

Eq. (4.6) means that flutter wind speed for the full-scale bridge is estimated by multiplying the measured wind speed with a factor of 1.14.

6.4 3D Elastic Model Test of Tower at Erection Stage

6.4.1 Description of Test

The aerodynamic stability of the tower at erection stage was investigated by a three dimensional elastic model test, as shown in Figures 6.8 and 6.9.

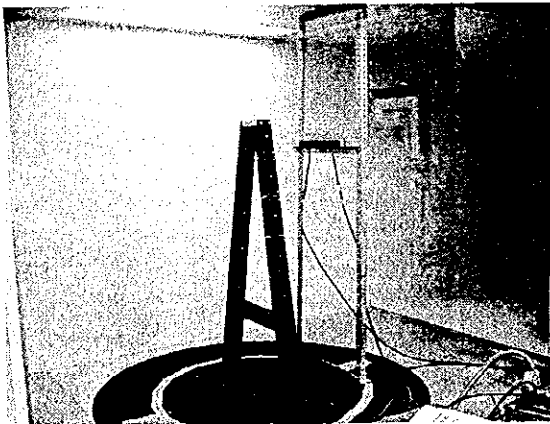


Figure 6.8 3D Elastic Tower Model and Laser Displacement Meters (Wind angle: 90 degrees)

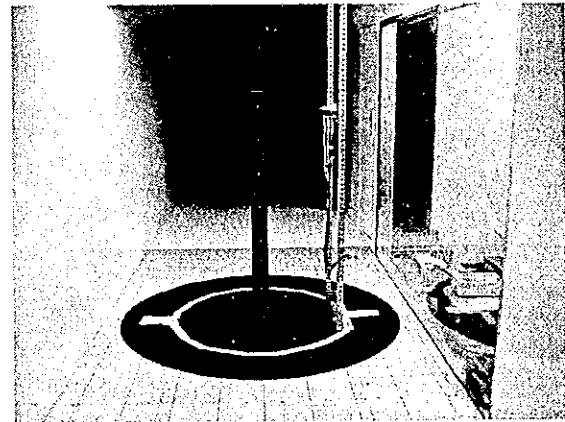


Figure 6.9 3D Elastic Tower Model (Wind angle: 0 degree)

The model consists of steel covers and steel elastic beams inside. The beams represent the stiffness of the full-scale structure based on the similarity requirement. The covers reproduce the physical shape of the full-scale structure. Both of them reproduce the weight distribution.

The tower is inverse Y shape and made by concrete. Since it was feared that an erection-stage tower before two shafts are connected would be most unstable aerodynamically, the wind-tunnel test was carried out with that stage tower model. The scale of the model is 1/95 which is corresponding to 122-m height in the full-scale.

Based on the tower erection plan, the two tower shafts are connected to each other at the top during erection period, aerodynamic vibration out of plane of the tower is basically measured with changing wind flow angle (β) (see Figure 6.10) as well as wind speed in the wind tunnel.

Test cases are shown in Table 6.5.

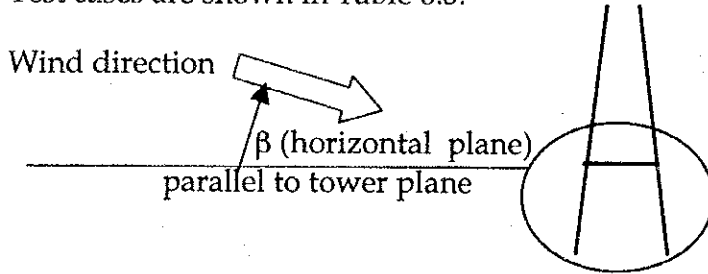


Figure 6.10 Wind Flow Angle: β

Table 6.5 Test Cases of Wind-Tunnel Test of Tower

Wind flow	Flow angle: β (degree)	Connection at tower top	Direction of vibration measured
Smooth flow	0	connected	Out-of-plane
	10		
	20		
	30		
	45	Not connected	Out-of-plane & In-plane
	60		
	90		

As for the similarity requirements, the same conditions as those in the case of deck were imposed. That is,

- (1) Inertia parameter: $m/(\rho D^2)$
- (2) Elastic parameter: $U/(fD)$
- (3) Damping parameter: δ_s

In order to obtain the wind-speed ratio between the test and the full-scale, eigenvalue analysis of the tower at erection stage was executed. Analytical conditions are shown in Table 6.6. The results of natural frequencies and fundamental vibration modes are shown in Table 6.7 and Figure 6.11.

The wind-speed ratio is given by

$$\frac{U_p}{U_m} = 95 \frac{f_p}{f_m} \quad (5.1)$$

where U and f are wind speed and frequency, respectively. The subscripts p

and m represent the full-scale and test, respectively.

Table 6.6 Analytical Conditions in Eigenvalue Analysis

		Section A	Section B
Unit weight (tf/m)	m	94.89	42.17
Stiffness of cross section (m ⁴)	I_x	76.75	107.25
	I_y	183.8	91.85
	J	192.99	130.81
Young modulus (tf/m ²)	E	3.30E+06	3.30E+06
Shear modulus (tf/m ²)	G	1.40E+06	1.40E+06
Section area (m ²)	A	37.96	16.87
Height (m) (above basement)		about 122	

Table 6.7 Natural Frequencies of Tower at Erection Stage

Model No.	Frequency (Hz)	
	Real	Model
1	0.4447	0.9426
2	0.5143	0.9690
3	0.5153	1.0040
4	0.5290	1.1100
5	2.3180	4.7690
6	2.6290	5.0450
7	2.7770	5.7540
8	3.4460	6.1580
9	4.8820	9.3000
10	5.3140	11.2000
11	6.3470	13.4400
12	8.6560	16.3500
13	9.1550	18.9200
14	9.4910	20.6400
15	10.3000	21.1200
16	10.7000	45.5500
17	11.7900	29.9400
18	11.9500	34.0900
19	15.6000	34.6000
20	19.4800	41.9000

Note: frequencies (real) and (model) represent natural frequencies analyzed with the full-scale dimensions and model dimensions, respectively.

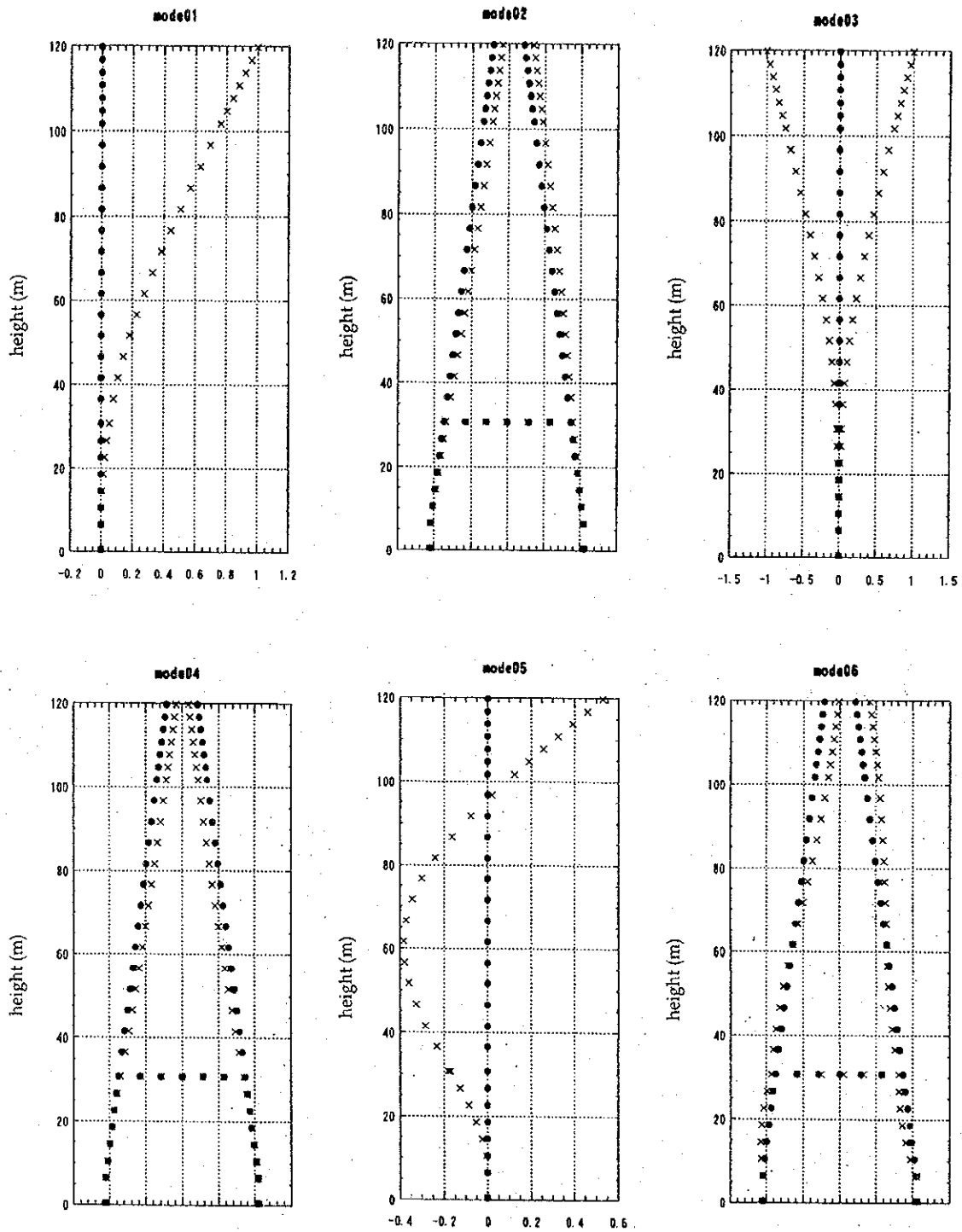


Figure 6.11 Fundamental Vibration Modes of Tower at Erection Stage

6.4.2 Test Results

Natural frequencies and structural damping measured in test cases are shown in Table 6.8. These frequencies are used calculating the wind-speed ratio.

Table 6.8 Natural Frequencies and Structural Damping

Flow angle (deg.)	Mode 1		Mode 3		Mode 4	
	Natural frequency (Hz)	Structural damping	Natural frequency (Hz)	Structural damping	Natural frequency (Hz)	Structural damping
Connected at tower top						
0	-	-	-	-	-	-
10	-	-	-	-	-	-
20	7.54	0.017	-	-	-	-
30	7.58	0.012	-	-	-	-
45	7.57	0.018	-	-	-	-
60	7.54	0.021	-	-	-	-
90	7.56	0.024	-	-	-	-
Ave.	7.56	0.018	-	-	-	-
Not connected at tower top						
0	7.53	0.012	10.38	0.005	-	-
10	-	-	-	-	-	-
20	7.59	0.017	10.44	0.004	-	-
30	7.55	0.016	10.40	0.005	-	-
45	7.56	0.017	10.31	0.004	-	-
60	7.53	0.015	10.40	0.006	-	-
90	7.57	0.016	10.36	0.004	10.05	0.002
Ave.	7.56	0.016	10.38	0.005	10.05	0.002

Note: Modes 1, 3 and 4 correspond to the mode shapes shown in figure 5.4. Mode 1 is 1st out-of-plane bending, mode 2 1st torsion and mode 4 1st in-plane bending.

Structural damping measured range from 0.012 to 0.024 in log decrement for mode 1, from 0.004 to 0.006 for mode 2 and 0.002 for mode 4. Honshu-Shikoku Bridge Authority specifies structural damping for tower at erection stage as 0.01 in log decrement [2.1]. The values measured are slightly higher than the specification. However, considering that many temporary structures such as scaffold are attached on the tower at erection stage and relatively low tower height, it is judged that the damping measured are in allowable range.

Aerodynamic responses of the tower top versus wind flow angle and wind speed are shown in Figures 6.12 - 6.19.

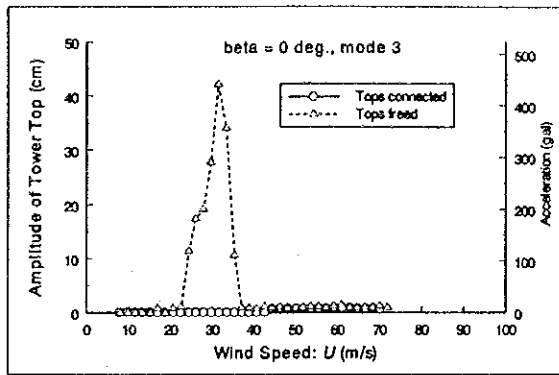
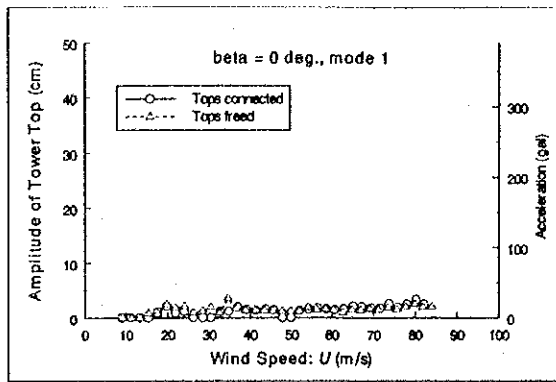


Figure 6.12 Diagram of Tower Top Response versus Wind Speed ($\beta = 0$ deg.)

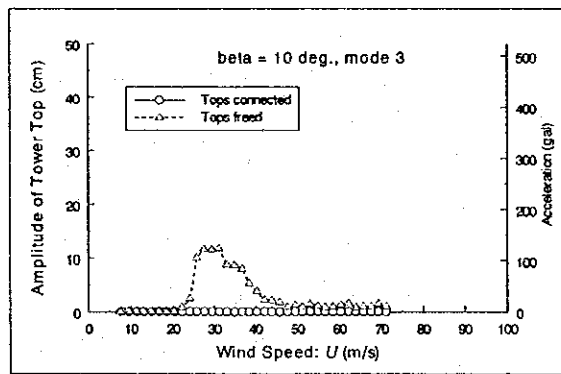
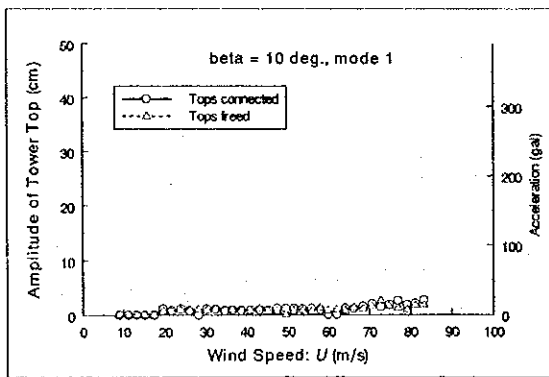


Figure 6.13 Diagram of Tower Top Response versus Wind Speed ($\beta = 10$ deg.)

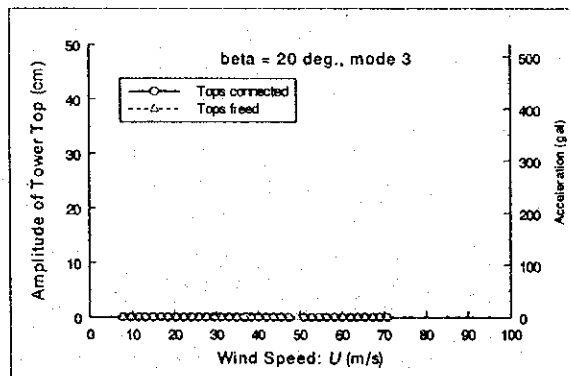
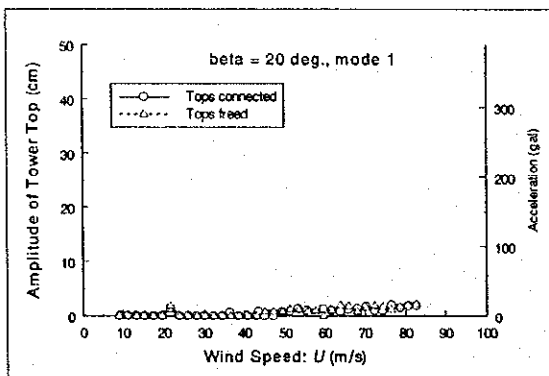


Figure 6.14 Diagram of Tower Top Response versus Wind Speed ($\beta = 20$ deg.)

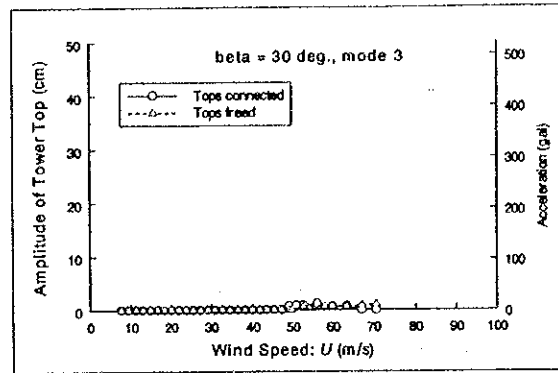
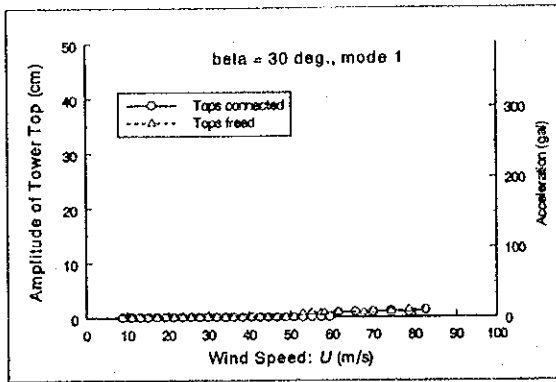


Figure 6.15 Diagram of Tower Top Response versus Wind Speed ($\beta = 30$ deg.)

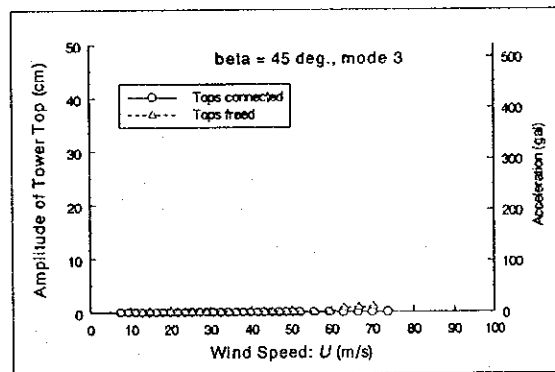
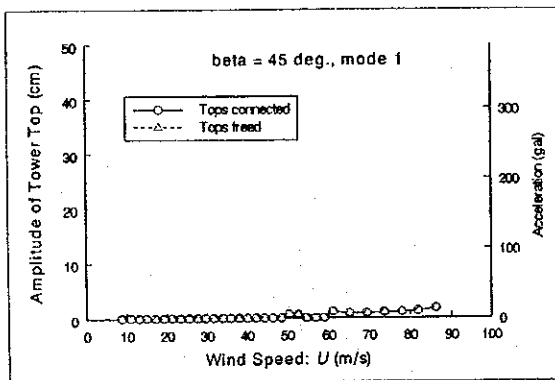


Figure 6.16 Diagram of Tower Top Response versus Wind Speed ($\beta = 45$ deg.)

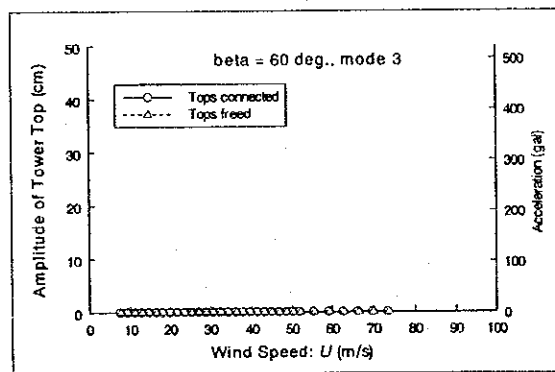
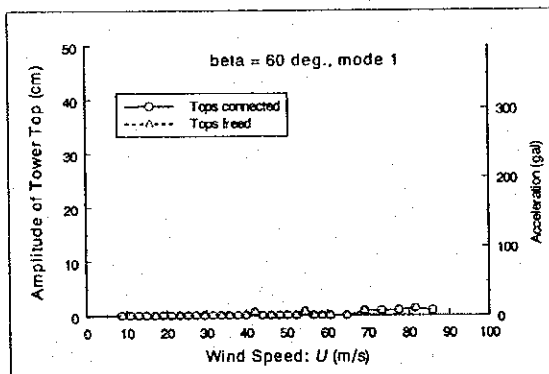


Figure 6.17 Diagram of Tower Top Response versus Wind Speed ($\beta = 60$ deg.)

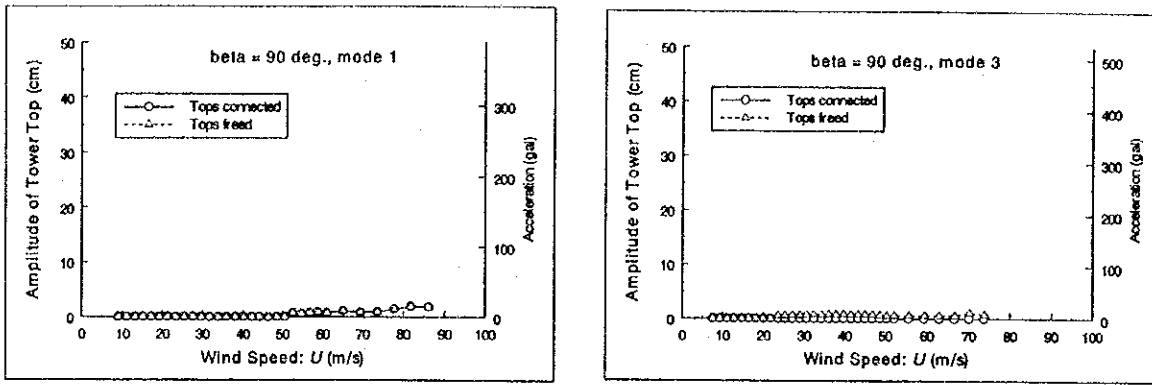


Figure 6.18 Diagram of Tower Top Response versus Wind Speed ($\beta = 90$ deg.)

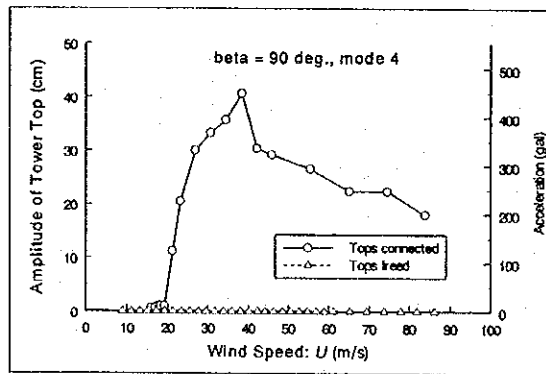


Figure 6.19 Diagram of Tower Top Response versus Wind Speed ($\beta = 90$ deg., in-plane vibration)

6.4.3 Judgment of Aerodynamic Stability of Tower at Erection Stage

The reference wind speed at 10 m, U_{10} is specified as 40 m/s for the Can Tho Bridge. Based on U_{10} , the design wind speed for the tower at erection stage is calculated as follows [2.1 & 4.1]:

The reference height of the tower is given as the 65 % height of the tower, which is 79 m (= 122 × 0.65). Assuming the power law for wind-speed profile and the power of 0.16 (ground roughness category: II), the design wind speed for the tower at erection stage of the Can Tho Bridge is calculated as

$$U_D = 40 \times \left(\frac{79}{10} \right)^{0.16} = 56 \text{ m/s} \quad (5.2)$$

The verification wind speed for divergent vibration is defined as follows:

$$U_{vf} = 1.2 \times U_D = 1.2 \times 56 = 67 \text{ m/s} \quad (5.3)$$

It is quite natural that design wind speed and verification at an erection period be reduced, because the erection period is short. There are two methods to decide the design wind speeds at erection stage.

One is that an equivalent wind speed giving the wind load half of completed-stage value is defined as an erection-stage value. That is, 0.71 × design wind speed at a completed stage is one at an erection stage. The other one is that a wind speed giving the exceeding probability same as one at a completed stage is defined as an erection-stage value.

Using the second method with an erection period of 2 - 3 years, the factor of an erection stage is calculated as around 0.6, which is smaller than 0.71 from the first method. In this research, in order to give large safety margin, the first method (0.71) is used.

After all, the design wind speed of the tower at erection stage is:

$$U_{DE} = 0.71 \times U_D = 0.71 \times 56 = 40 \text{ m/s} \quad (5.4)$$

and the verification wind speed for divergent vibration is:

$$U_{vE} = 0.71 \times U_{vf} = 0.71 \times 67 = 48 \text{ m/s} \quad (5.5)$$

Referring to the specified values above, the judgment of the aerodynamic stability of the tower at erection stage of the Can Tho Bridge is made below.

In the cases of the wind-flow angle being other than 0, 10 and 90 degrees, no

harmful vibration was observed.

In the cases of wind-flow angle of 0 and 10 degrees, torsional vibration was observed without the connection at the tower top and its amplitude was 42 cm and 12 cm at a wind speed of 30 m/s, respectively. Corresponding acceleration reaches 440 gal at 0 degree and 120 gal at 10 degrees. Those vibrations occurred below the design wind speed and its acceleration is not small. However, with connecting the tower top, those vibrations were completely suppressed. Connecting at the tower top will be an effective countermeasure to suppress vibration.

In the case of wind-flow angle of 90 degrees, out-of-plane bending and torsional vibration did not occur with/without the connection at the tower top. However, in-plane bending vibration with amplitude of 41 cm occurred at a wind speed of 39 m/s if not connected at the tower top. Connecting the tower top completely suppressed the vibration.

From the results above, it is concluded that without the connection at the tower top, large-amplitude vibrations of torsion at 0 & 10 degrees and of in-plane at 90 degrees would occur, however with the connection at the tower top, no vibration would occur. It is also concluded that there would not occur harmful problem with connecting the tower top during construction.

6.5 Wind-induced Vibration and Countermeasures of Stay Cables

6.5.1 Wind-Induced Vibration of Stay Cables

Wind-induced vibration observed at stay cables of cable-stayed bridges is often classified into

- (1) Vortex-induced vibration
- (2) Rain-wind-induced vibration
- (3) "High-wind-speed-induced vibration"
- (4) Wake galloping

Vortex-induced vibration is caused by well-known Karman vortices formed after a round-shape cable. It is usually observed at relatively low wind speed and is easily suppressed with small additional damping. Since a buffer rubber for anti angle bend installed at cable fixing points, vortex-induced vibration disappeared in many cases.

Rain-wind-induced vibration is thought to occur with a wind flow and water rivulets on the cable surface which deforms the cable cross section to wind-susceptible. It was pointed out that a relatively strong axial flow along the leeward cable axis plays an important role. Rain-wind-induced vibration with large amplitude has been observed at many cable-stayed bridges. Damping devices such as an oil damper and rubber damper are often used to suppress the vibration.

"High-wind-speed-induced vibration" (name is not formally recognized) has been reported to occur at a relatively high wind speed (30 - 40 m/s) [7.1]. There are many unknown facts to be investigated, however. It is difficult to include the investigation and its countermeasure in this study.

Wake-galloping is observed at parallel cables. The leeward cable vibrates with large amplitude. If the Can Tho Bridge has single-plane cables, this study does not need to deal with wake-galloping.

From the facts above, rain-wind-induced vibration (and wake galloping if necessary) will be the utmost concern in the design stage.

[Rain-Wind-Induced Vibration]

Figure 6.20 shows the wind-tunnel-test results (responses of rain-wind-induced vibration) of stay cables of a cable-stayed bridge with a center span length of about 900 m [7.2]. The test was executed with three conditions of cable frequency. The longer the cable is, the lower the frequency is. It is seen that the onset wind speed of vibration except for 1st peak with $f = 0.45$ Hz is

about 10 m/s in three cases. This means that cable frequency does not affect the onset wind speed. Since rain-wind-induced vibration is caused by water rivulets on the surface as well as wind, onset wind speed of rain-wind-induced vibration is governed by the change of cross-section shape.

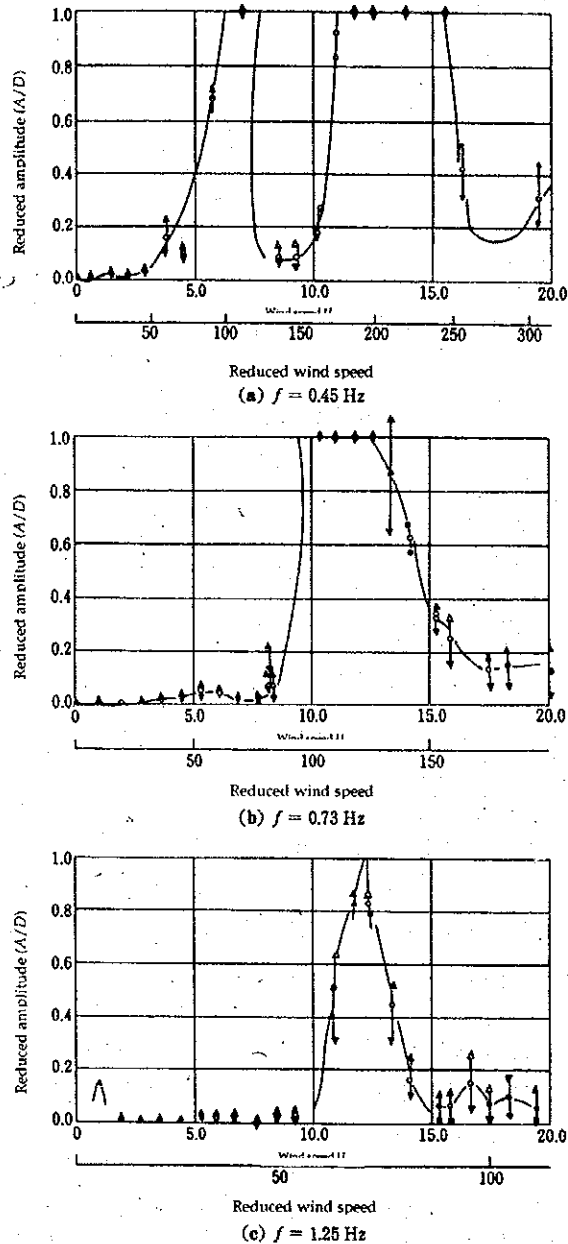


Figure 6.20 Relationship of responses of rain-wind-induced vibration and frequency [7.2]

In fact the response from a wind-tunnel test changes at about 10 m/s, as shown in Figure 6.21, which corresponds the change of the water rivulet pattern on the cable surface [7.2].

Figure 6.22 shows the relationship between the onset wind speed of rain-

wind-induced vibration and Scruton number (S_c) [7.3]. From this result, $S_c = 60$ is the minimum requirement to suppress the vibration. Another report says that cable damping in log decrement of 0.02 (approximately equal to $S_c = 60$) is required to suppress. These values are recommended as a reference for the Can Tho Bridge. However, the latest and detailed information is necessary.

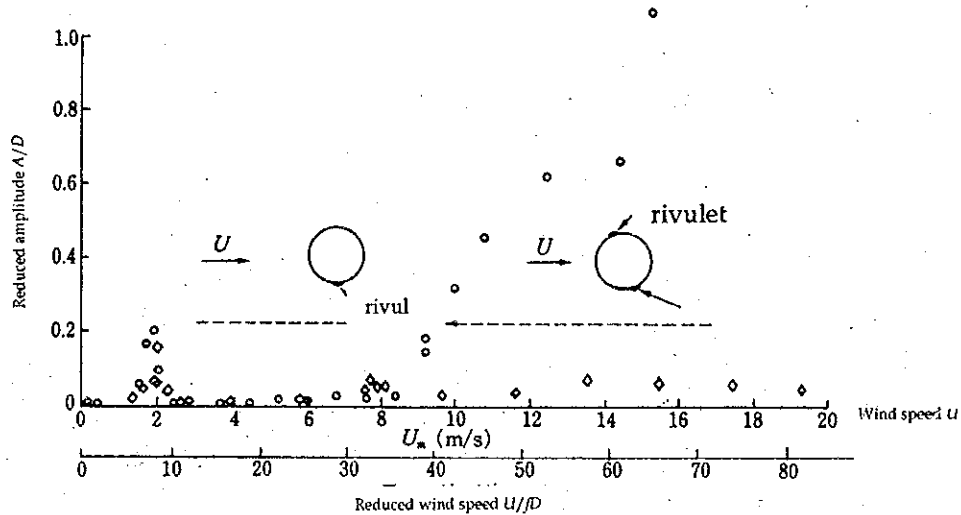


Figure 6.21 Responses of Rain-Wind-Induced Vibration and Position of Water Rivulets against Wind Speed [7.2]

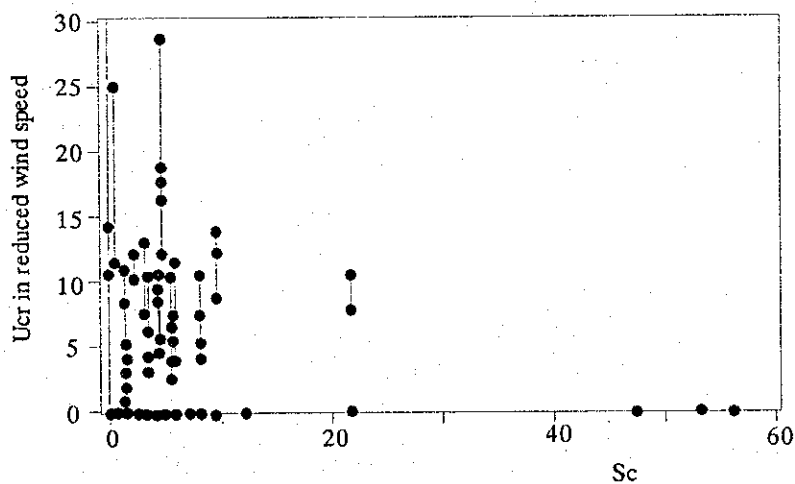


Figure 6.22 Relationship between Onset Wind Speed of Rain-Wind-Induced Vibration and Scruton Number [7.3]

6.5.2 Countermeasures of Wind-Induced Vibration of Stay Cables

There are three types of countermeasures to suppress wind-induced vibration of stay cables.

- (1) Connecting cables to each other at intermediate position(s)

(This is understood that connecting cables makes natural frequency high and increase the onset wind speed.)

- (2) Damping devices

- (3) Change of cable shape or surface

(Making strips, indents on the surface changes aerodynamic characteristics)

Historically, the method of connecting cables has been applied and the effectiveness was recognized to a certain degree. However, mechanical problem at connecting points such as breaking connecting wire has often been reported.

Second method with dampers is the most commonly used these days. But disadvantage of this method is that dampers are expensive and They need regular maintenance.

Recently a new idea of the third method has developed. There are three types of the change of cable surface. First [7.4] is to make indents on the cable surface randomly and applied at the Tatara Bridge as shown in Figure 6.23. Usually, making patterns on a round shape cable increases roughness and drag. However, adjusting patterns such as one of the Tatara Bridge keeps drag as low as that of a round cable. Second [7.5] is to change the cable cross section as shown in Figure 6.24. This idea is based on the prevention of forming water rivulets on the surface. This cable was applied at the Higashi Kobe Bridge. However, the cable yield large drag coefficient of 1.2. The last [7.6] is to make U-shape strips on the surface as shown in Figure 6.25. This cable was applied at the Yuge Bridge.

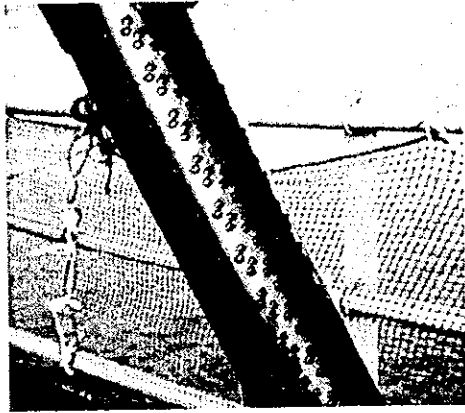


Figure 6.23 Indent Cable of Tataro Bridge

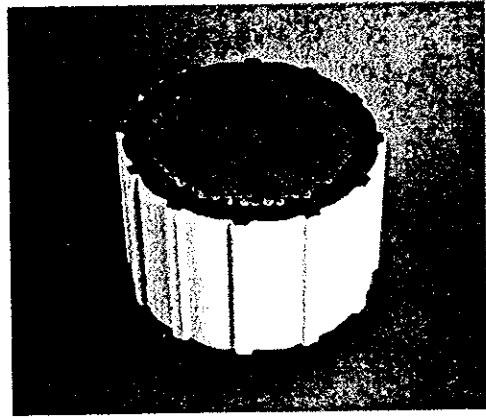


Figure 6.24 Protuberance Cable of Higashi Kobe Bridge



Figure 6.25 U-Shape Stripe Cable of Yuge Bridge

6.5.3 Recommendation for Cable Vibration of Can Tho Bridge

Vortex-induced vibration is anticipated to occur, however, installing anti-angle-bend rubber buffers at cable fixing points (commonly used in large cable-stayed bridges) will suppress the vibration.

If the bridge adopts parallel or multi cables in one plane, wake galloping will inevitably occur without appropriate cable distance. In this case, appropriate cable distance or allocation is the most important.

It is not easy to judge in advance whether rain-wind-induced vibration would occur or not at the bridge site. Recommendations for rain-wind-induced vibration of the Can Tho Bridge are as follows:

- (1) After cable erection without any countermeasures, vibration monitoring is to be carried out.
- (2) In case that the vibration would occur during the monitoring, countermeasure(s) is to be taken. If no vibration is observed, judgment that rain-wind-induced vibration would not occur at the Can Tho Bridge is to be made. (Since the vibration is relatively easy to occur

with conditions of a wind speed of about 10 m/s and rain, the vibration is likely to be observed in a short period.)

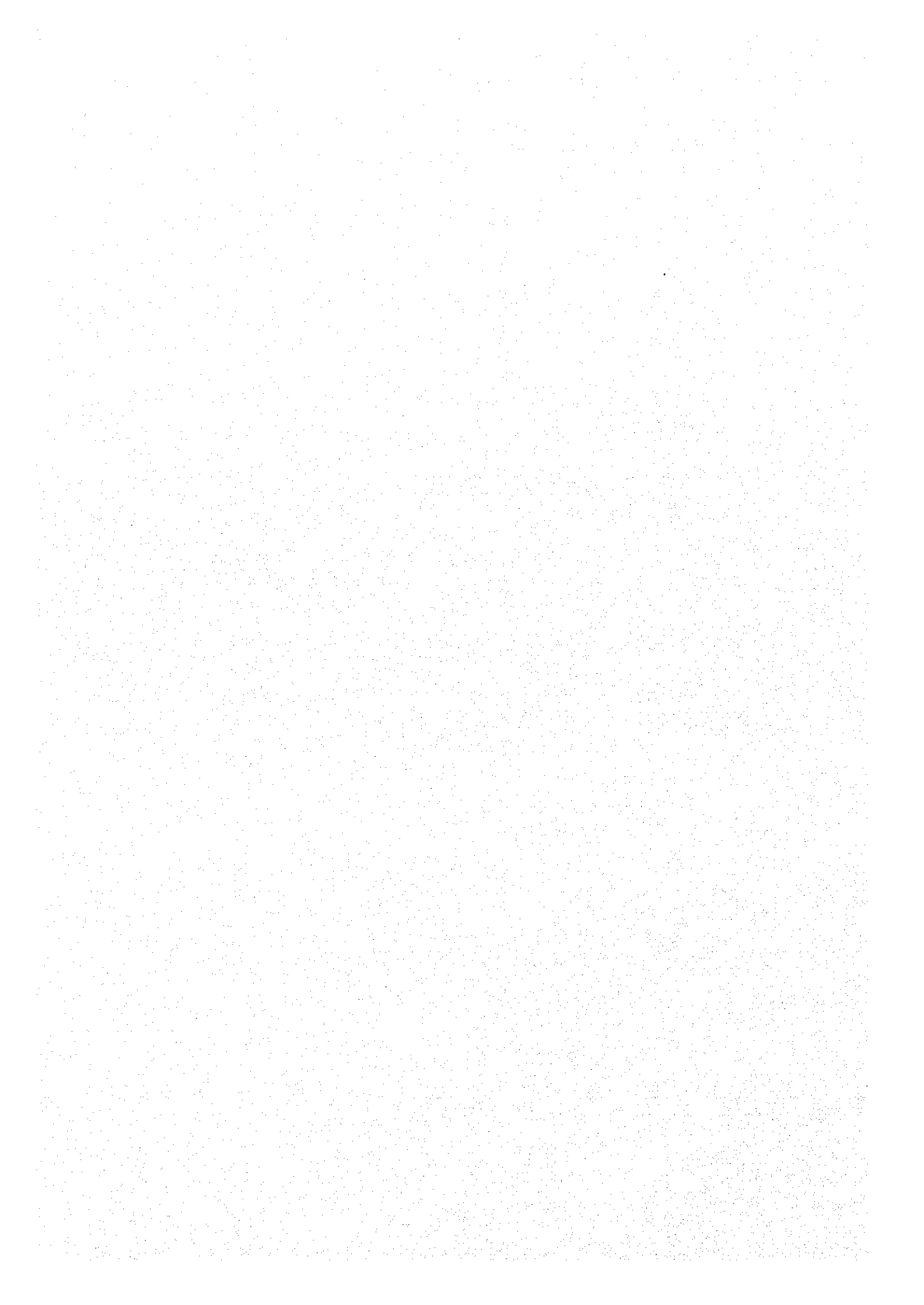
- (3) Even in case that the vibration would occur, there is one solution that no countermeasure is taken. However, the vibration is often accompanied by quite large amplitude (≥ 1 m). So it will be proper to take some kind of countermeasures.

Since countermeasures are taken after cable erection, damping devices will be the only option left.

- (4) Specifications of damping devices such as required damping level can be referred to the description in this chapter. The Central Miko Bridge with a center span length of 590 m, which is the same level as that in this bridge, installed damping devices to suppress cable vibration. It will be a reference to the countermeasure of cable vibration of the Can Tho Bridge.

Chapter 7

DETAILED DESIGN



CHAPTER 7 DETAILED DESIGN

7.1 Drainage System related to Opening of Bridge and Box Culvert

7.1.1 Methodology

The methodology for this Study consists of the following stages:

(1) Data collection includes:

- Meteorological data on hourly, daily and monthly rainfall patterns
- River gauging stations providing annual peak river heights and discharges
- Sub-institute for Water Resources Planning
- The Regional Road Maintenance Units which provided maintenance reports on previous flood behavior
- Interviews with local residents
- Consultant Reports associated with hydraulic works in the Mekong Delta

(2) Determination of design criteria is referred to Vietnamese standards and Ministry of Transport and Communication Notices

(3) Verification of data: It was necessary to confirm a good correlation between the data from the above sources. Where there was poor correlation, the cause needed to be determined so that inappropriate data could be eliminated from the analysis.

(4) Hydrological Analysis - The main component of this work was a flood discharge analysis, using Manning Equation to determine design flood discharge and levels.

(5) Hydraulic Analysis includes:

- Determining the required drainage system
- Determining the backwater

7.1.2 Inundation around the Bridge Site

According to the F/S, the flood inundation area in 1984, 1992, and 1993 is described below:

- (1) In the 1984 flood, the maximum water level was 2.0m and its duration was 3 to 5 months at Can Tho.
- (2) During the past three years, the whole area of An Giang and Dong

Thap provinces were inundated. In 1984 and 1992 Kien Giang, Can Tho, Vinh Long, and Tien Giang provinces were almost flooded, and 50% of the Long An, Tra Vinh, and Soc Trang provinces were flooded. The inundation area of Ben Tre province was relatively small. Also, in 1994 about 50% of Kien Giang, Can Tho, Vinh Long, Tien Giang, and Long An provinces were flooded.

- (3) When comparing 1984 and 1992 inundated areas, paddy fields of Tra Vinh were classified as flooded areas in 1992. The rest of the areas were similar to the 1984 classification. This was probably due to the similarity in the water level pattern, and it was observed that the monthly average maximum water level change showed a similar pattern according to the measurements at the Can Tho measuring station.
- (4) From the water depth comparison for the years 1984 and 1994 where data was available, it was found that the water depth of the inundated area was above 1 meter for locations up to 120 km away from the estuary. This area was in the vicinity of Long Xuyen, and northwest of the upper catchment. However, a water depth of more than 0.5 meters in 1984 covered the whole area of Hau river, and was only 15 km away from the Can Tho bridge site.

7.1.3 Estimate of Discharge

All box culverts and bridges crossings of the Project area are located on the relatively straight reaches of channel with uniform geometry upstream and downstream of bridge site, and it causes of constant cross section, roughness and slope, satisfy. The Manning Equation to determine the discharge is available.

$$Q = \frac{AR^{2/3}S^{1/2}}{n}$$

Where

A - area (m²) of cross section of flow

R - hydraulic radius = A/WP (m)

WP - wetted perimeter (m) of the cross-section of flow

S - hydraulic slope (m/m)

n - Manning roughness coefficient

Based on the Manning Equation with design water levels, cross section of the streams, hydraulic slope, and the roughness coefficients, the discharges of all streams at bridge sites and box culverts are determined and are summarized

in the Table 7.1.

Table 7.1 Bridges and Box Culverts

Bridges				Box Culverts			
No.	Name	Chainage (km)	Discharge (m ³ /s)	No.	Box culvert	Chainage (km)	Discharge (m ³ /s)
1	Tra Va Large	0+ 711	445.300	1	Box culvert	0 + 416	12.65
2	Tra Va Small	1 + 910	168.630	2	Box culvert	1 + 063	7.00
3	Tra On	3 + 718	539.155	3	Box culvert	1 + 300	7.00
4	Cai Tac 1	8 + 551	67.387	4	Box culvert	1 + 560	6.92
5	Cai Tac 2	9 + 450	29.57	5	Box culvert	2 + 150	15.00
6	Cai Da	10 + 463	133.29	6	Box culvert	2 + 620	16.00
7	Ba Mang	11+215	66.902	7	Box culvert	2 + 835	15.00
8	Cai Nai	12 + 383	164.43	8	Box culvert	3 + 170	16.16
9	Ap My	13 + 180	80.225	9	Box culvert	4 + 125	5.00
10	Cai Rang	13 + 936	223.75	10	Box culvert	4 + 318	8.00
Total			1918.64	11	Box culvert	4 + 640	13.50
				12	Box culvert	7 + 820	6.00
				13	Box culvert	7 + 950	7.00
				14	Box culvert	8 + 820	15.3.
				15	Box culvert	9 + 760	6.00
				16	Box culvert	10 + 310	6.40
				17	Box culvert	10 + 690	7.00
				18	Box culvert	10 + 950	6.47
				19	Box culvert	11 + 451	7.00
				20	Box culvert	11 + 690	7.00
				21	Box culvert	11 + 976	5.95
				22	Box culvert	12 + 180	7.00
				23	Box culvert	12 + 592	3.79
				24	Box culvert	12 + 756	8.00
				25	Box culvert	13 + 600	23.18
				26	Box culvert	14 + 247	5.40
				27	Box culvert	14 + 450	4.00
				28	Box culvert	14 + 625	5.00
				29	Box culvert	14 + 890	3.00
				Total			255.72

7.1.4 Opening of Bridge and Box Culvert

The required openings are determined by the discharge of the rivers or canals. This is based on an empirical regime formula (Lacy's formula) for stable alluvial channels:

$$W_s = CQ^{1/2}$$

Where W_s is the net waterway surface width at design discharge, Q is the design discharge and C is a coefficient. This formula was originally proposed by Lacey for sand - bed canals and river. The suggested range indicated on the chart is from $C = 1.8$ to $C = 2.7$. The upper end of the range should be used for shifting channels in sandy materials, but for relatively stable channels in more scour - resistant materials the lower end may be used, subject to confirmation from local experience. Further adjustment of the waterway opening width should be made on economic condition after consideration of scour and other factors. The width to be adopted may be determined from the range indicated by Figure 7.1 waterway opening widths and cross sectional areas should always be calculated normal to the principal direction of flow as it enters the bridge in major flood.

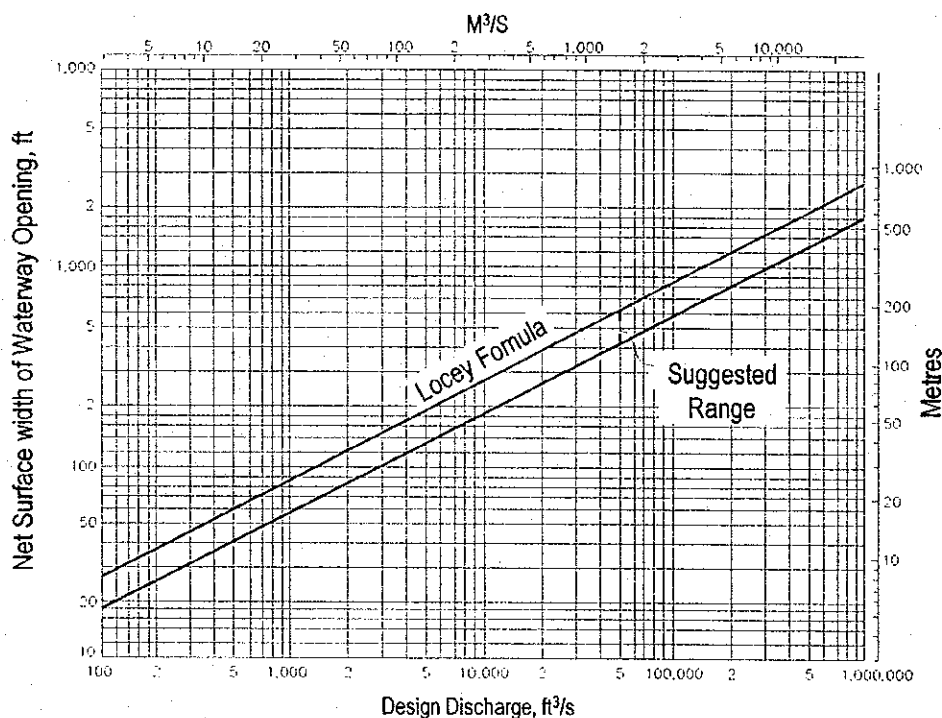


Figure 7.1 Chart for Selecting a Trial Waterway Opening Width Based on Lacey's Regime Formula for Alluvial Channels

Based on the determined discharges, the openings that cross over the rivers or canals on flood plains at both sides of the Hau River are selected and listed in the Table 7.2. The calculation results of discharge, opening and cross-section are shown in Table 7.3 and 7.4, respectively.

Table 7.2 Relief Openings on Floodplains at Both Sides of the Hau River

No.	Name of relief opening	Station (Km)	Design water level H (m)	Design discharge (m/s)	Normal relief opening	Skew angle 0°	Cost	Proposed relief opening	Net waterway surface width (m)
1	Tra Va Large	0 + 711	1.9	445.3	125	40	0.766	163	62
2	Tra Va Small	1 + 910	1.89	168.63	56	17	0.925	60	30
3	Tra On	3 + 718	1.87	539.155	115	40	0.766	150	83
4	Cai Tac1	8 + 551	1.86	67.38	36	25	0.906	40	33
5	Cai Tac2	9 + 450	1.87	29.57	40	44	0.72	30	18
6	Cai Da	10 + 463	1.88	133.29	58	7	0.9925	60	55
7	Ba Mang	11 + 215	1.89	66.9	38	0	1	22	18
8	Cai Nai	12 + 383	1.91	164.43	60	0	1	60	50
9	Ap My	13 + 180	1.92	80.22	46	23	0.92	50	50
10	Cai Rang	13 + 936	1.93	223.75	75	33	0.83	90	80

Table 7.3 Designed Openings of the Approach Road Sections Calculating According to Discharge

Side	No.	Station (km)	Name	Discharge Estimated (m ³ /s)	Required Opening (m)	Design Opening (m)	Total Discharge (m ³ /s)	%
VinhLong	1	0 + 416	box culvert	12.65	4	5	17	0.051
	2	0 + 711	<u>Tra va large Bridge</u>	445.3	163	195	454.35	1.370
	3	1 + 063	box culvert	7	2.2	5	13	0.039
	4	1 + 300	box culvert	7	2.2	5	13	0.039
	5	1 + 560	box culvert	6.92	1.75	3	12	0.036
	6	1 + 910	<u>Tra va small bridge</u>	168.63	60	76.9	182.58	0.550
	7	2 + 150	box culvert	15	3.6	5	20	0.060
	8	2 + 620	box culvert	16	3.85	5	20	0.060
	9	2 + 835	box culvert	15	3.65	5	19	0.057
	10	3 + 170	box culvert	16.16	3.85	5	19	0.057
	11	3 + 718	<u>Tra on bridge</u>	539.155	150	189	549.655	1.657
	12	4 + 125	box culvert	5	2.4	5	10	0.030
	13	4 + 318	box culvert	8	1.3	10	62	0.187
	14	4 + 640	box culvert	13.5	1	6.5	32	0.096
	Subtotal			1275.315	402.8	520.4	1423.585	4.291
Can Tho	15	6 + 285	<u>Main bridge</u>	31,000	1,824	2,615	31,367.91	94.550
	16	7 + 820	box culvert	6	1	3	18	0.054
	17	7 + 950	box culvert	7	1.2	5	28	0.084
	18	8 + 551	<u>Cai tac 1 bridge</u>	67.38	40	160	94.11	0.284
	19	8 + 820	box culvert	15.3	1.35	5	50	0.151
	20	9 + 450	<u>Cai tac 2 bridge</u>	29.57	30	37.1	32.314	0.097
	21	9 + 760	box culvert	6	2	5	15	0.045
	22	10 + 310	box culvert	6.4	2.2	5	15.5	0.047
	23	10 + 463	<u>Cai Da bridge</u>	133.29	60	88	137.07	0.413
	24	10 + 690	box culvert	7	2.6	5	13	0.039
	25	10 + 950	box culvert	6.47	2.4	5	13.5	0.041
	26	11 + 215	<u>Ba mang bridge</u>	66.9	22	25.1	67.62	0.204
	27	11 + 451	box culvert	7	3	5	12.5	0.038
	28	11 + 690	box culvert	7	3.5	5	10	0.030
	29	11 + 976	box culvert	5.95	3.4	5	8.6	0.026
	30	12 + 180	box culvert	7	3.6	5	8.7	0.026
	31	12 + 383	<u>Cai nai bridge</u>	164.43	60	89	171.17	0.516
	32	12 + 592	box culvert	3.79	2.3	5	6.99	0.021
	33	12 + 756	box culvert	8	1	5	40	0.121
	34	13 + 180	<u>Ap My bridge</u>	80.22	50	123	88.19	0.266
	35	13 + 600	box culvert	23.18	4	5	75	0.226
	36	13 + 936	<u>Cai rang bridge</u>	223.75	90	225	251.296	0.758
	37	14 + 247	box culvert	5.4	1.5	5	18	0.054
	38	14 + 450	box culvert	4	2.2	5	9.5	0.029
	39	14 + 625	box culvert	5	1.3	5	19.5	0.059
	40	14 + 890	box culvert	3	1.4	5	11	0.033
		Subtotal			899.03	391.95	835.2	1214.56
TOTAL (Including Main Bridge)				33,174	2,618.75	3,970.6	34,006.10	102.51
TOTAL (excluding Main Bridge)				2,174.34	794.75	1,355.6	2,638.15	121.33

Table 7.4 Designed Opening of the Approach Road Section Calculating according to Opening

Side	No.	Station (km)	Name	Discharge (m ³ /s)	Required Opening (m)	Net Design Opening (m)	%
Vinh Long	1	0 + 416	Box culvert	12.65	4	5	0.19
	2	0 + 711	<u>Tra va large bridge</u>	445.3	163	195	7.45
	3	1 + 063	Box culvert	7	2.2	5	0.19
	4	1 + 300	Box culvert	7	2.2	5	0.19
	5	1 + 560	Box culvert	6.92	1.75	3	0.11
	6	1 + 910	<u>Tra va small bridge</u>	168.63	60	76.9	2.94
	7	2 + 150	Box culvert	15	3.6	5	0.19
	8	2 + 620	Box culvert	16	3.85	5	0.19
	9	2 + 835	Box culvert	15	3.65	5	0.19
	10	3 + 170	Box culvert	16.16	3.85	5	0.19
	11	3 + 718	<u>Tra on bridge</u>	539.155	150	189	7.22
	12	4 + 125	Box culvert	5	2.4	5	0.19
	13	4 + 318	Box culvert	8	1.3	10	0.38
	14	4 + 640	Box culvert	13.5	1	6.5	0.25
		Subtotal		1275.315	402.8	520.4	19.87
Can Tho	15	6 + 285	<u>Main Bridge</u>	31000	1824	2615	99.86
	16	7 + 820	Box culvert	6	1	3	0.11
	17	7 + 950	Box culvert	7	1.2	5	0.19
	18	8 + 551	<u>Cai tac 1 bridge</u>	67.38	40	160	6.11
	19	8 + 820	Box culvert	15.3	1.35	5	0.19
	20	9 + 450	<u>Cai tac 2 bridge</u>	29.57	30	37.1	1.42
	21	9 + 760	Box culvert	6	2	5	0.19
	22	10 + 310	Box culvert	6.4	2.2	5	0.19
	23	10 + 463	<u>Cai Da bridge</u>	133.29	60	88	3.36
	24	10 + 690	Box culvert	7	2.6	5	0.19
	25	10 + 950	Box culvert	6.47	2.4	5	0.19
	26	11 + 215	<u>Ba mang bridge</u>	66.9	22	25.1	0.96
	27	11 + 451	Box culvert	7	3	5	0.19
	28	11 + 690	Box culvert	7	3.5	5	0.19
	29	11 + 976	Box culvert	5.95	3.4	5	0.19
	30	12 + 180	Box culvert	7	3.6	5	0.19
	31	12 + 383	<u>Cai nai bridge</u>	164.43	60	89	3.40
	32	12 + 592	Box culvert	3.79	2.3	5	0.19
	33	12 + 756	Box culvert	8	1	5	0.19
	34	13 + 180	<u>Ap My bridge</u>	80.22	50	123	4.70
	35	13 + 600	Box culvert	23.18	4	5	0.19
	36	13 + 936	<u>Cai rang bridge</u>	223.75	90	225	8.59
	37	14 + 247	Box culvert	5.4	1.5	5	0.19
	38	14 + 450	Box culvert	4	2.2	5	0.19
	39	14 + 625	Box culvert	5	1.3	5	0.19
	40	14 + 890	Box culvert	3	1.4	5	0.19
			Subtotal		899.03	391.95	835.20
TOTAL (including Main Bridge)				33,174.35	2,618.75	3,970.60	151.62
TOTAL (excluding Main Bridge)				2,174.34	794.75	1,355.60	170.57

The main Can Tho bridge conveys the discharge of 31,000m³/s which occupied 93.45% of the total flood discharge of Hau river (31,000 + 2,174.36 = 33,174.36m³/s). The bridges and box culverts on floodplain convey the discharge of 2,174.36m³/s which occupied 6.55% of the total discharge.

The discharges for the designed bridges and box culverts were estimated in accordance with the Manning Equation, $Q = \frac{1}{n} A R^{2/3} S^{1/2}$. The openings were also estimated through the Lacey's formula for alluvial channels. The cross section areas were calculated based on the opening of bridges and box culverts and flood water level.

The design opening by the bridges and culverts in accordance with discharge and opening area are summarized in Table 7.5.

Table 7.5 Summary of Design Discharge and Design Opening

Location	Estimated Discharge (m ³ /sec)	Design Discharge (m ³ /sec)	Required Opening (m)	Design Opening (m)
(a) Vinh Long side	1,275 (100%)	1,423 (111%)	403 (100%)	520 (129%)
(b) Main Bridge	31,000 (100%)	31,367 (101%)	1,824 (100%)	2,615 (143%)
(b) Can Tho Side	899 (100%)	1,214 (135%)	391 (100%)	835 (213%)
(c) Total	33,174 (100%)	34,006 (102%)	2,618 (100%)	3,970 (151%)

The table shows that the design discharge is greater than the estimated one by 2%. The design opening is greater than the required one by 51%.

7.1.5 Backwater at the Bridge Location

Backwater refers to the raising of flood water levels, as a result of the constricting or obstructing effects of bridges as associated road approaches. The height by which the flood level is raised at any point is referred to as "backwater".

The expression for backwater has been formulated by applying the principle of conservation of energy between the point of maximum backwater upstream from the bridge and a point downstream from the bridge at which normal stage has been re-established.

The expression is reasonably valid if the channel in the vicinity is essentially

straight, the cross-sectional area of the stream is fairly uniform, the gradient of the bed is approximately constant in the reach of bridge site, the flow is free to contract and expand, there is no appreciable erosion of the bed in the constriction due to scour, and the flow is in the sub-critical range.

The expression for computation of backwater upstream from a bridge constriction is as follows:

$$h_1^* = k^* \alpha_2 \frac{V^2 n_2}{2g} + \alpha_1 \left[\left(\frac{An_2}{A_4} \right)^2 - \left(\frac{An_2}{A_1} \right)^2 \right] \frac{V^2 n_2}{2g}$$

where:

h_1^* - Total backwater height (m)

k^* - total backwater coefficient

α_1 and α_2 kinetic energy coefficient

$$\alpha_1 = \frac{\Sigma(qv^2)}{QV_1^2} \quad \alpha_2 = \frac{\Sigma(qv^2)}{QV_2^2}$$

An_2 - gross water area (m²) in constriction measured below normal stage

Vn_2 - average velocity (m/s) in constriction or Q/An_2

A_4 - Water area (m²) at section 4 where normal stage is re-established

A_1 - total water area (m²) at section 1 including that produced by the backwater

Can Tho bridge crosses the Hau river at a straight reach, the channel is large and deep, conveying most of the discharge (31,000 m³/s) composed to the total one (33,174 m³/s).

Gradient of the bed is approximately constant, the flow is free to contract and expand.

Based on this condition and backwater expression, the backwater of Can Tho bridge and all relief bridges on the approach embankment have been determined. They are shown in Table 7.6 and Figure 7.2.

Table 7.6 Backwater of Can Tho Bridge and All Relief Bridges

Name of bridge	Can Tho	Cha Va 1	Cha Va 2	Tra On	Cai Tac 1	Cai Tac 2	Cai Da	Ba Mang	Cai Nai	Ap My	Cai Rang
Backwater h^*1 (m)	0.043	0.054	0.0254	0.0287	0.022	0.01	0.04	0.0193	0.019	0.017	0.0227

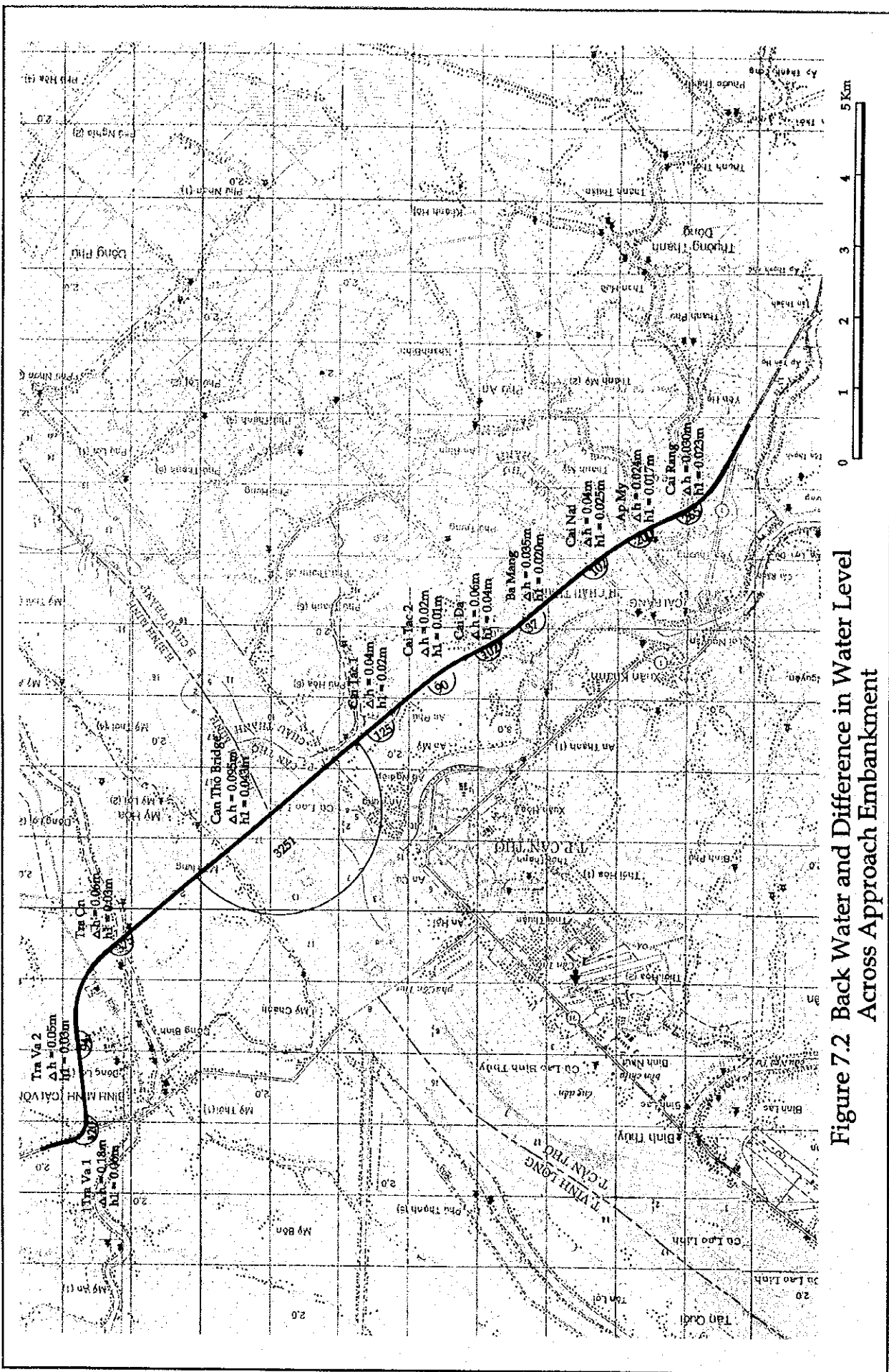


Figure 7.2 Back Water and Difference in Water Level Across Approach Embankment

7.1.6 Interview Survey on the Past Inundation

Due to the complication of flooding in the Can Tho tidal region, the Study Team found it to be impossible to analytically or statistically determine flood levels. It was, therefore concluded that the best and most practicable approach to obtaining suitable flood data would be to undertake a detailed flooding history interview survey at the Project site.

At the end of August 1999 the Study Team undertook a field survey to the Can Tho bridge and all relief bridges on its floodplains component of the Project. The survey covered the 15km stretch from the Cha Va Bridge to a location approximately 2 km south of Cai Rang bridge where the new road crossed the existing road.

The Can Tho bridge and its approach embankments traverse a flat agricultural area with mainly rice fields. There are many waterways in the area, many of which are being used for inland water transportation. For consideration lengths of the Project, the new road runs adjacent to the canals. The water table is high. However, most of the bridges have a high vertical clearance, which raises the road lightly above the surrounding area so it is not affected by the high water table.

In the field survey, the high water level marks of 1978, 1991, and 1997 floods have been located by local people who has been living in the vicinity of the proposed bridge site.

Also in the field survey, the discussion on drainage system of the Project area with local staff of agriculture and rural development of Vinh Long and Can Tho Department has been made.

The interview survey was done in the 19 points at site to presume the flood water depth and level of 1978, 1991, and 1997 floods, and the results were summarized in Table 7.7.

Table 7.7 The Surveyed Point of High Water Marks

The surveyed points	1978				1991				1997			
	Water level (m)	Water depth (m)	Duration (h)	Direction	Water level (m)	Water depth (m)	Duration (h)	Direction	Water level (m)	Water depth (m)	Duration (h)	Direction
1	1.51	0.26	2-3h	Flow downstream	1.42	0.17	2-3h	Flow downstream	1.32	0.07	2-3h	Flow upstream
2	1.48	0.16	-	-	1.42	0.10	-	-	1.35	0.03	-	-
3	1.66	0.31	-	-	1.40	0.05	-	-	1.40	0.05	-	-
4	1.70	0.32	-	-	1.50	0.12	-	-	1.84	0.46	-	-
5	1.53	0.43	-	-	1.58	0.48	-	-	1.33	0.23	-	-
6	1.46	0.36	-	-	1.41	0.31	-	-	1.35	0.25	-	-
7	1.64	0.54	-	-	1.51	0.41	-	-	1.67	0.57	-	-
8	1.63	0.31	-	-	1.52	0.20	-	-	1.68	0.36	-	-
9	1.63	0.28	-	-	1.53	0.18	-	-	1.70	0.35	-	-
10	1.64	0.29	-	-	1.53	0.18	-	-	1.57	0.22	-	-
11	1.55	0.15	-	-	1.48	0.08	-	-	1.70	0.30	-	-
12	1.54	0.24	-	-	1.45	0.15	-	-	1.49	0.19	-	-
13	1.28	0.08	-	-	1.25	0.05	-	-	1.43	0.23	-	-
14	1.32	0.12	-	-	1.27	0.07	-	-	1.45	0.26	-	-
15	1.51	0.13	-	-	1.42	0.04	-	-	1.63	0.25	-	-
16	1.51	0.46	-	-	1.11	0.06	-	-	1.68	0.63	-	-
17	1.53	0.13	-	-	1.43	0.03	-	-	1.64	0.24	-	-
18	1.55	0.19	-	-	1.44	0.08	-	-	1.62	0.27	-	-
19	1.69	0.26	-	-	1.52	0.09	-	-	1.85	0.42	-	-

Notes:

- The water level of points far from the Hau riverbank is lower
- Generally, the 1991 flood water level are lower than the one of 1978 about 8-12cm while the 1997 flood water level have the highest values.
- In the 1978 and 1991 floods the flow downstream while the 1997 flood, the flow upstream.
- The duration of peak flood is about 2-3 hours but after lowering 40-50cm the flood level existing more than 20 days.

The characteristics of these big floods are described below:

(1) The 1978 flood

The water level rose from the middle of August and reached its highest point of 1.63m at Can Tho bridge site. Water level in the estuary and along the river was not high, due to low tide during peak flood.

The 1978 flood in the Mekong Delta had two peaks with one month span.

The first flood increased rapidly and occurred early in the last 10 days of August. It was strongly regulated by the Great Lake and depression areas along Mekong River which were still empty.

The second flood occurred at the end of September which was assessed as a low flood in Laos but as a high flood in lower part of Mekong Delta because of the following reasons:

- The regulation capacity of the Great Lake and of the depressed areas along the Mekong River was used already by the first flood.
- The second flood came when the first one had not been drained out yet.
- High spring tide.
- Heavy rainfall in the delta.

(2) The 1991 flood

In the second 10 days of August, water level in Hau River rose rapidly. At the bridge site, water level was higher than 1.1m on 25 September and reached a maximum level of 1.52m on 27 October.

The 1991 flood in the Mekong Delta had two peaks with one month span. The first peak was higher than the second peak in the upper part of the delta and the first peak was lower than the second one in the lower part of the delta.

It was classified as a big flood in terms of magnitude and as a normal flood in terms of time.

(3) The 1997 flood

The 1997 flood was a small one in upstream part of the Mekong Delta, but it was influenced by a typhoon and sea level, therefore the water level at the bridge site was relatively high, it was approximate the design water level of a 100-year return period. Within the Project area, there is a meteorological station at Can Tho. Also within the Project area, there is a river gauging station. This station is located about 3km upstream of Can Tho bridge site.

7.1.7 Review of the 2000 Flood

At the end of the Detailed Design Stage (September and October 2000), a flood occurred at the Mekong Delta, and large areas including the Project site were affected.

The Study Team strongly suggested the review of this flood data at the beginning of the next stage. Moreover, if necessary, the design works will be amended after considering this flood data before the pre-construction procedures.